A performance modelling study for zero fossil CO_2 stack operation and solvent thermal reclaiming in post-combustion capture industrial applications

Stavros Michailos[a,*], Mathieu Lucquiaud[b], August D Benz[c], Daniel Mullen[d], William Elliott[e], Jon Gibbins[b]

[a]School of Engineering, University of Hull, Hull HU6 7RX, UK
[b]Department of Mechanical Engineering, The University of Sheffield, Sheffield S3 7RD, UK
[c]Private Consultant, Burlingame, CA 94010, USA
[d]SSE Thermal, One Forbury Place, 43 Forbury Road, Reading, RG1 3JH, UK
[e]Bechtel National, Inc., 12011 Sunset Hills Rd, Reston, VA 20190, USA

Abstract

Post-combustion capture (PCC) of CO_2 is widely recognised as the most mature technology to mitigate CO_2 emissions from existing fossil fuel-based power plants and industrial sources, and successful deployment will predominantly rely on the ability of the PCC plant to consistently achieve high capture fractions.

To this end, the performance modelling study presented herein is the first attempt to identify engineering options for long-term, cost-effective windows for zero fossil CO_2 stack emission PCC operation, when 100% of the added fuel CO_2 (100% of the fossil CO_2) is captured, in key industrial applications including combined cycle gas turbine (CCGT) power plants, steel, cement, energy from waste (EfW) and oil refining (fluidised catalytic crackers). Further, low-cost designs for effective solvent recovery through thermal reclaiming with effective energy recovery are analysed for the first time for non-proprietary, open-art aqueous MEA solvent at 35% w/w (unloaded).

At 100% capture of the added fuel CO_2, low lean loadings (between 0.1-0.12 molCO_2/molMEA) enhance mass transfer in the absorber while a raised desorber pressure of 2.4 bar limits excessive energy consumption. In fact, for an absorber packing height of 20m (2 x 10m beds), the optimum specific reboiler duty (SRD) to capture 100% of the added fuel CO_2 (zero fossil CO_2 stack operation) was found to lie between 3.62 and 3.96 GJ/tCO_2, while for a 3 x 8m bed absorber, i.e. 24m, the SRD drops to 3.46 -3.75 GJ/tCO_2; both cases, well within the range of reported energy penalty for 90-95% capture, which has significantly higher residual CO_2 emissions.

Further, we analysed two strategies of continuously operating a thermal reclaimer, I.e., single stage and two-stage reclaiming system (the 1st operates at stripper pressure while the 2nd one at atmospheric) with effective energy integration and consideration of both volatile and non-volatile components. Two-stage reclaiming can substantially reduce water addition compared to single stage reclaiming from 100-400% of the reclaimer solvent flow to 0-50%. Yet, there exists a trade-off, namely the greater the MEA recovery, the greater is the uptake of volatile thermal degradation products. For example, in the case of single stage reclaiming operation, for ~90% MEA recovery approximately 35% of the HEEDA is recycled to the PCC and when MEA recovery increases to ~95%, the associated HEEDA return reaches ~52%. Effective integration of thermal reclaiming with the desorber results in a small additional electricity output penalty, i.e. ranging from 0.3 to 1.13% relative to the output with capture but with no reclaiming. But it should be noted that a solvent management technique is essential to an amine based PCC as accumulation of degradation products will affect capture efficiency and associated energy costs, and eventually will be a showstopper.

Overall, the study suggests that industrial applications fitted with PCC can achieve deep decarbonisation in a cost-efficient manner with effective solvent degradation remedial strategies and contrary to the consensus that high capture fractions are associated with excessive energy penalties. Hence, the results can provide meaningful information for engineering deployment and policy decision making.

1. Introduction

In the quest for mitigating climate change and ensuring a sustainable future, the imperative to reduce greenhouse gas emissions has never been more pressing. The commitment set by many governments across the globe for net-zero has designated Carbon Capture and Storage (CCS) as a necessity and not an option. Post-Combustion Capture of CO_2 (PCC) using amines will be likely the most widely used flue gas capture technology. For example, two out of the three capture projects, to receive funding from the UK government as part of the Track-1 CCS Cluster Sequencing process, will be amine-based PCC plants [1] . PCC offers the advantage of retrofitting existing infrastructure, making it a practical and cost-effective option for reducing emissions from a variety of existing industrial applications, and is also being considered for new-build applications (Track 1 new builds), including steam methane reformers [2].

Up until recently, the conventional wisdom has been – largely because it was a 'standard' baseline used in studies comparing costs – that capturing 90% of the CO_2 in a flue gas stream was both good enough and the best that could be done to minimise the cost per tonne of CO_2 captured, see Brandl et al.[3] for a history of capture levels. But, to help deliver net-zero fossil CO_2 stack operation (or 100% of the added fuel CO_2 or 100% fossil CO_2 capture), combustion applications fitted with PCC should ideally operate at such a manner that the whole amount of the fossil CO_2 added to the air is captured and hence the vented gas should contain the same amount of CO_2 as the combustion air; this entails gross capture fraction from the flue gas of at least 99% up to ~99.8%, depending on the industrial application.

According to a recent United Kingdom BAT Guidance [4], a review of best available technologies (BAT) [5] suggests that PCC designs should target CO_2 capture fractions of 95% or higher. To this direction, solvent suppliers, such as Mitsubishi [6], and academics [3, 7, 8] have reported on the feasibility of ultra-high capture fractions. A detailed commentary on these studies can be found in [9]. However, most high capture studies have utilised process parameters that were optimised for lower capture fractions (e.g. 90%) and in particular lean loadings such as 0.2 $molCO_2/molMEA$[7, 8] that resulted in either high specific reboiler duty (SRD), i.e. >4 GJ/tCO_2 or excessive absorber packing heights of more than 40m. For example , Brandl et al.[3] calculated that for 99% capture, the capital cost of the absorber (and by inference, the packing height) was increased significantly from the 95% value, but this was for a assumed constant lean loading of 0.15 $molCO_2/molMEA$; relationship between packing height and lean loading was not reported.

To address the lack of a thorough investigation on the effect that key process parameters have on ultra-high capture fractions, the authors in a previous modelling study on CCGT flue gas [9] demonstrated that lean loadings below 0.15 $molCO_2/molMEA$ coupled with a slightly elevated desorber pressure can achieve reasonable energy penalties, <4 GJ/tCO_2, for zero fossil CO_2 stack operation. Low lean loadings result in relatively low liquid-to-gas (L/G) ratios and absorber packing heights within the range of industrial standards (20-24m) designed for 90%-95% capture; hence no additional CAPEX investment is required for typically the most expensive PCC equipment. In addition, low liquid flows are expected to have a positive effect on the marginal cost (e.g. heat exchangers and desorber) of increasing capture levels up to 100% in PCC plant compared to designs for 95% capture and assist in derisking capital recovery. In this regard, Mullen and Lucquiaud [10] have applied the proposed design and estimated that the marginal cost of CO_2 avoided from 95% capture to 100% fossil CO_2 capture is 184 £/tCO_2 for a CCGT, which is lower than current estimates for direct air capture costs.

Reclaiming is essential to maintain the capture efficiency of the PCC plant and avoid undesirable effects such as foaming, corrosion and increased viscosity. Solvent reclaiming units have been reported in pilot testing campaigns but in general they lack details about operating windows, energy penalty and solvent recovery. Endo et al. [11] and Hirata et al. [12] reported that successful operation of reclaiming of MHI KS-1 solvent has been repeatedly carried out and that no critical issues such as fouling and corrosion have been found. A steam heated thermal reclaimer operating semi-continuously has been tested for Fluor's Econamine FG Plus^{SM} (EFG+) Technology that is integrated with the PCC desorber; the EFG+ reclaimer operates at lower pressure and temperature compared to typical reclaiming technologies [13]. The Hitachi H3-1 Solvent has been tested at the National Carbon Capture Center (NCCC) facilities in which a thermal reclaimer has been integrated to the desorber and caustic soda was added to degrade the heat stable salts and release the solvent [14]. Further, there exist few modelling studies regarding thermal reclamation. Garg et al. [15] have utilised Aspen Plus to model an MEA thermal reclaiming unit operating at vacuum of 0.067 bar and temperatures of 110-130°C; nevertheless, the purpose of the study was to conduct high level cost estimations and as such the study does not include detailed energy and material balances as well as investigation of different reclaiming techniques. Similarly, Putta et al. [16], as part of performing a techno-economic assessment of a PCC coupled to a Natural Gas Combined Cycle (NGCC) power plant, have modelled in Aspen Plus an MEA thermal reclaiming unit that uses caustic treatment to neutralize acids and release the solvent; the unit operates at stripper pressure and the vapour stream returns to the PCC desorber. Nevertheless, this study also lacks detailed quantification of energy and mass flows and analysis of alternative reclaiming configurations.

The current research aims at identifying from a process modelling perspective modifications needed to PCC designs to be able to capture 100% of the added fuel CO_2 from flue gases derived from a variety of industries. The latter include steel, cement, energy from waste (EfW) and oil refinery fluidised catalytic cracker units (FCC). The PCC design is based on previous modelling work presented by the authors in[9] and focuses on low leadings (<0.13 $molCO_2/molMEA$) and desorber pressure of 2.4 bara. In this regard, the study estimates key process parameters such as lean loading, liquid to gas ratio (L/G), packing height, and intercooling for each case. Further, as the solvent should be reclaimed to ensure long-term cost-effective PCC operation and due to the fact that the increased desorber pressures (hence temperatures) may increase thermal degradation, a simplified degradation model has been developed based on operational data from Technology Centre Mongstad (TCM) and this has been used to analyse two thermal reclaiming configurations in Aspen Plus to estimate solvent recovery rates, the concentration of the degradation products due to the increase of degradation rates of operating at higher temperatures and the additional energy penalty aiming at minimising the latter through heat integration .

Unlocking the full potential of PCC is of paramount importance for the success of CCS at scale and this study suggests for the first time operational envelopes for zero fossil CO_2 stack operation that can be used in test programmes and plant design studies.

2. Framework of the study

2.1 Methods

Material and energy balances have been established through process modelling in Aspen Plus V12.1 using the add-on MEA Steady State Model developed by the DOE Carbon Capture Simulation Initiative (CCSI). The CCSI process model is tuned and validated against data from the PCC unit at the National Carbon Capture Centre (NCCC) in Wilsonville, Alabama. More information about the thermodynamics, mass transfer correlations and the kinetics of the CCSI toolkit can be found in [17].

Figure 1 is the process flow diagram (PFD) of a typical amine-based absorption-desorption PCC plant and this configuration has been utilised herein. MEA at 35% concentration (unloaded) absorbs CO_2 from the flue gas in the absorber in a counter flow manner. Then, the rich solvent recovers heat from the bottom stream (hot lean) of the desorber and enters at the top of the desorber in which CO_2 is stripped by adding heat to the reboiler. The design assumes that the flue gases are saturated at 45°C in a cooler, water is removed and then pressure boosted by a fan to roughly 1.1 bar. A water wash on the top of the absorber is a standard design practice but this has not been included in this study as it does not affect the CO_2 capture process.

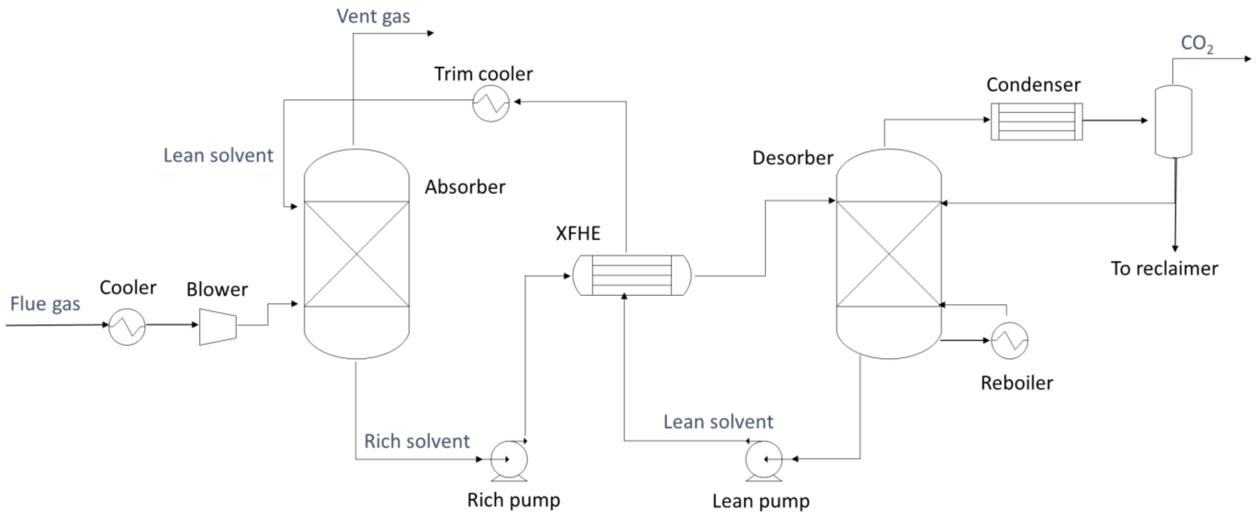

Figure 1. Process flow diagram of the PCC plant as implemented in Aspen Plus.

A key feature of this study is that it considers low lean loadings to enhance mass transfer at the absorber, <0.13 molMEA/molCO_2, obtained efficiently with slightly elevated desorber pressure, 2.4 bar. The authors have shown [9] that there exists an inflection point for the lean loading, at different desorber pressures, below which the SRD increases sharply (see **Figure 2**), the higher the pressure the lower the lean loading at the inflection point, which in turn allows for higher capture fractions at the absorber. For a dry CO_2 concentration of 4.19% v/v, a capture fraction of 95% and a desorber pressure of 2.4 bar, as depicted in **Figure 2,** the inflection point is observed at 0.13 molMEA/molCO_2. Similarly, for this study that examines flue gases from a variety of industrial applications the goal is to identify the inflection point required at ultra-high capture fractions. Key data to run the PCC simulations has been received either from industrial partners or relevant literature [18]; this data along with key design assumptions are presented in **Table 1**. Further, for a given height and lean loading, the solvent flowrate for all cases (including intercooling scenarios) to the absorber was manipulated to achieve the desired CO_2 capture fraction. The reboiler duty of the desorber was calculated in order to achieve the specified lean loading of the absorber inlet. The cross-heat flow exchanger is designed with a temperature approach at the hot side of ~10°C while the desorber reboiler was sized based on LP steam at 3.15 bar, 135°C [19]. Finally, the diameters of the columns (absorber and stripper) were calculated for an 80% approach to flooding. Absorber heights of 20m and 24m have been tested as these represent current industrial standards for 95% capture and the study aims at demonstrating that no significant design modifications are required to efficiently increase the capture fraction to 100% of the fossil CO_2 contained in the flue gas. Further, based on information from industrialists (co-authors of the study) absorber beds can reach a maximum of 10m and hence for the 20m absorber two identical beds are utilised (10 m each) while for the 24m three identical beds of 8 m each; when intercooling is applied, of necessity this is done between the 2 beds for the 20m case and in between the top and the middle bed in the 24m case (as mass transfer reduces at the top of the absorber).

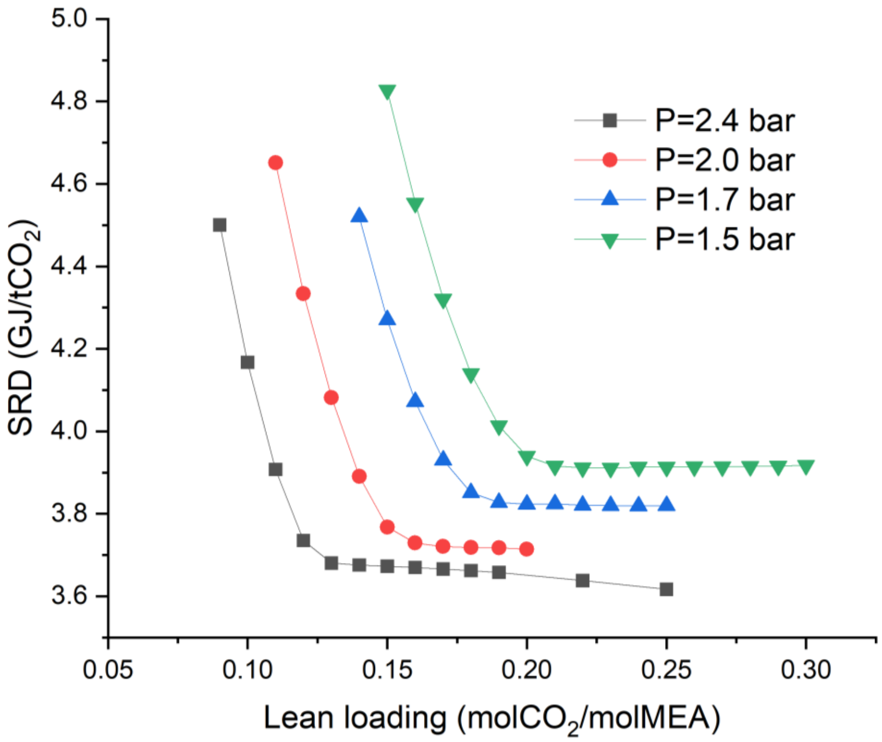

Figure 2. The SRD as a function of the lean loading and the desorber pressure (P). The capture fraction is 95% and the rich loading is 0.446 molCO$_2$/molMEA. Reproduced from [9]. Available under a Creative Commons Attribution License (CC BY). Copyright © 2022 Michailos and Gibbins.

Figure 3 depicts the PFD of the thermal reclaiming unit. This study analyses two configurations, i.e. 1-stage and 2-stage reclaiming. The first reclaimer operates at desorber pressure, and the resultant vapour is sent to the bottom of the desorber to recover the energy while the second reclaimer operates at atmospheric pressure (same as the absorber) and the resultant vapour stream, after removing impurities and recovering MEA, is sent to the top of the absorber for pressure control.

In the former, water is mixed with the solvent to control the reclaimer operating temperature, which is then heated, and the vapour stream is sent to the bottom of the desorber for energy and solvent recovery; the 1st reclaimer operates at desorber pressure, i.e. 2.4 bar. In the 2-stage configuration less water (compared to the 1-stage) is added to the 1st reclaimer and the vapour stream is sent again to the desorber; however, in this case the liquid bottom is mixed with additional water and heated to recover more solvent at the top of the 2nd reclaimer, which operates at atmospheric pressure. The vapour stream from the 2nd reclaimer is cooled and flashed, and the resulting liquid fraction containing water and recovered solvent is sent to the solvent tank while the flash gas is sent to the top of absorber; nitrogen (1.0 wt.%) is added to the low-pressure flash gas to ensure a small gas flow over to the absorber for pressure control. It should be noted that water is added to the reclaiming system as the resultant vapour (after heating) will reduce the partial pressure of the MEA, allowing it to distil out of the mixture at temperatures lower than its normal boiling point. The water added to the reclaiming stages is presented as % of the reclaimer feed (slipstream of the hot lean stream of the PCC) to give an insight of the overall reclaimer size. To minimise freshwater requirements, the additional water comes from the desorber condenser of the PCC; the PCC design assumes that 90% of the condensate returns to the top of the desorber while only a small fraction of the purged condensate (up to ~9%) is used for reclamation.

The liquids (residue) remaining in the 2nd stage reclaimer are sent for off-site disposal. For the 1-stage configuration, more water is utilised, up to 400% of the mass flow of the feed stream in the reclaiming process. In the 2-stage unit, water of up to 50% of the feed stream is added in the 1st reclaimer and an additional fixed amount of 30% is supplied to the 2nd reclaimer in order to minimise heat losses (as heat is only recovered at the 1st stage). Further, in order to limit degradation, reclaimer temperatures below 150°C, i.e. 135°C, 140°C and 145°C, have been used in modelling. Both typical oxidative and thermal degradation products have been considered to illustrate the effect of reclaiming conditions on other species than MEA and their concentrations have been estimated based on data from pilot campaigns reported in the Technology Centre Mongstad (TCM) [20]. As the study focuses on high capture fractions with increased reboiler pressure/temperatures and low lean loadings, approximate adjustments to the data of TCM have been made such as that degradation rates are assumed to double for every 8.5 to 10 K temperature rise (empirical rule based on the Arrhenius equation). Aiming at a conservative approach at calculating the degradation formation rates, we have assumed that for the oxidation rates for the investigated EfW absorber is the same as the TCM absorber although the O_2 content in the EfW flue gas is 8.7% (v/v) vs the 14.6% (v/v) in the TCM absorber [21]. For thermal degradation, we have neglected the effect of operating at lower carbamate concentration (i.e. low lean loading) that can hinder degradation rates. Further, Mullen et al. [22] have utilised the oxidative and thermal degradation reaction models of Braakhuis and Knuutila [23] and Braakhuis et al. [24], and showcased that the increase in oxidative degradation due to higher absorber height and thermal degradation due to higher reboiler pressure/temperature (135°C compared to 115°C) is between 23.7 and 138.8% which encourages the seemingly conservative assumption made herein that degradation rates double for every 10K rise.

The oxidative products include both organic and inorganic substances and they are assumed to undergo caustic treatment (with NaOH) prior to entering the reclaiming vessels to recover some of the degraded MEA by converting the Heat Stable Salts (HSS) to sodium salts. Liquid caustic is injected into the reclaimer feed stream in order to neutralize organic acids and release combined MEA for recovery within the reclaimer unit; average mass fractions of the organic and inorganic sodium salts (listed in the Supplementary Information) have been calculated based on Figure 6 in Morken et al. (2017); for modelling purposes sodium acetate and sulfate have been used to represent organic and inorganic sodium salts, respectively. Regarding thermal degradation, three main degradation products have been identified in the literature, i.e HEIA (1-(2-hydroxyethyl)-2-imidazolidone), HEEDA (N-(2-hydroxyethyl)-ethylenediamine) and 2-oxazolidone [25]. The calculation procedure herein estimated the overall generation of thermal degradation products and due to software limitations (e.g. absence of HEIA from the Aspen database), and lack of consistent composition breakdown of thermal degradation products, HEEDA ($C_4H_{12}N_2O$) was selected to represent conservatively the thermal degradation products (as the most volatile compound) and along with the inclusion in the model of the non-volatile sodium salts, they allow for more realistic vapour liquid equilibrium (VLE) calculations in the thermal reclaiming model. It should be noted that HEEDA is more volatile than HEIA and 2-oxazolidone, with boiling points of 240°C, 410°C [26] and 336°C (from Aspen Plus database) respectively, indicating that the model prediction regarding thermal degradation products carryover with the MEA vapour from the reclaimer is likely to be overestimated.

The EfW plant (for 100% capture of the fossil CO_2) is taken as an example to establish the mass and energy balances of the reclaiming unit for a 21-day inventory reclaiming cycle. This is around 0.11% (mass basis) of the hot lean flow (bottom stream of the desorber) directed to the reclaiming unit. Continuous reclaiming is considered, and so the equivalent of a full inventory of MEA is processed in 21 days; during this period the weight concentration of the degradation products and HSSs in the solvent is roughly 4.4 wt% and this is below the threshold of 5.74 wt%, at which the TCM plant was considered to still be fully operable. Detailed material balances for the reclaiming unit can be found in the Supplementary Information.

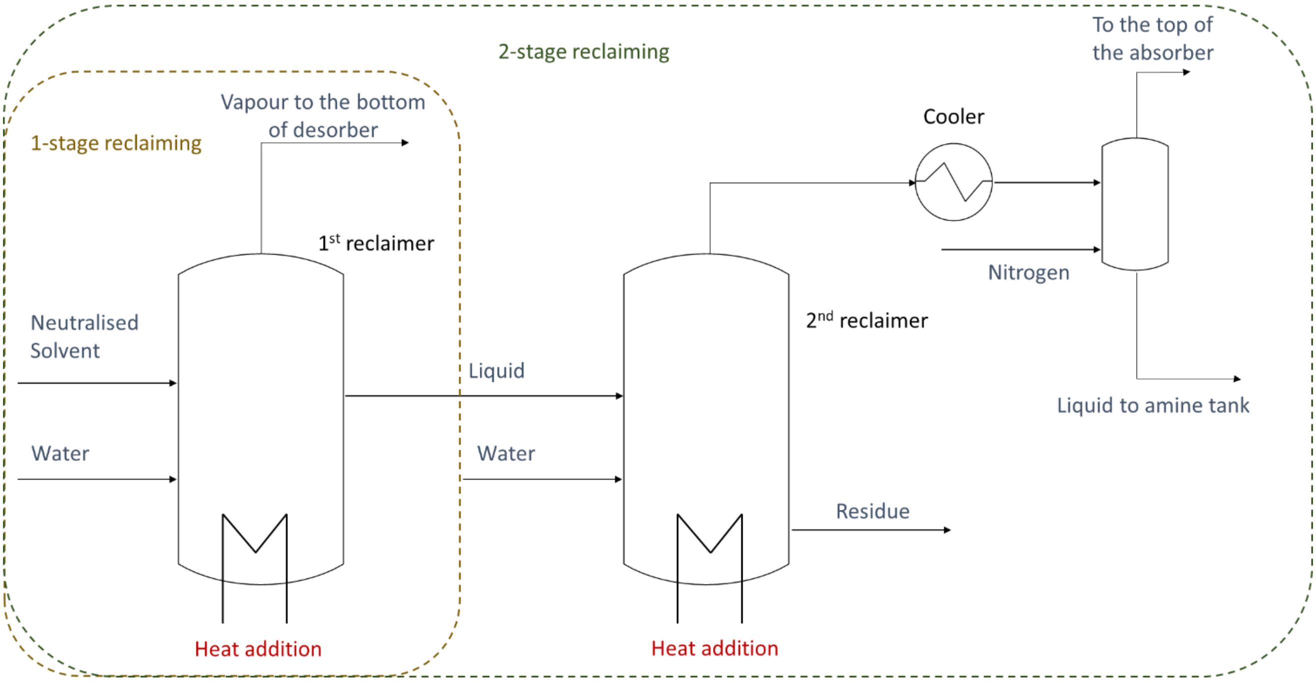

Figure 3. Process flow diagram of the thermal reclaiming configurations. Vapour from the 1st reclaimer is sent to the bottom of the desorber for energy recovery.

Table 1. Key input data for the PCC and the thermal reclaiming units.

Parameter	**Unit**	**Value**
PCC plant		
Flue Gas†		
Cement	kg/s	87.2
CCGT	kg/s	1012.9
EfW	kg/s	297.7
FCC	kg/s	87.2
Steel	kg/s	370.2
CO_2 dry concentration*		
Cement	v/v (%)	24.72
CCGT	v/v (%)	5.46
EfW	v/v (%)	11.12
FCC	v/v (%)	18.36
Steel	v/v (%)	28.41
Absorber height	m	20-24
Flue gas inlet temperature	°C	45
Lean Solvent Temperature to Absorber	°C	45
Desorber pressure	bara	2.4
MEA concentration (unloaded)	wt. %	35
Thermal reclaiming unit[×]		
Neutralised feed		
Water	kg/h	1177.82
CO_2	kg/h	59.47
MEA	kg/h	716.07
HEEDA[±]	kg/h	53.69
Sodium Acetate	kg/h	36.19
Sodium Sulfate	kg/h	4.81
1st reclaimer pressure	bara	2.4
2nd reclaimer pressure	bara	1.1

†Saturated at 45°C and pressure boosted to 1.1 bar

**Cement from [27], CCGT from industrial communications, EfW from industrial communications, FCC from [28], Steel from [29]*

× We have exemplified the design of the thermal reclaimer unit based on the EfW

± HEEDA is a proxy for all thermal degradation products

2.2 Limitations

Although the study serves as the first attempt to investigate modifications needed to efficiently achieve 100% capture of the added fuel CO_2 in key industrial applications and to analyse different configurations of thermal reclaiming and its integration with the PCC plant, there still exist limitations and areas that need further research. For example, due to limitations related to the Aspen Plus database and scarce data available regarding detailed breakdown composition of degradation products, only HEEDA has been used to approximate the thermal degradations products but as previously mentioned HEEDA's relatively higher volatility makes this assumption, if any, to result in conservative (overestimating) results regarding degradation uptake. Potential degradation of MEA during reclaiming at higher than desorber temperatures has not been considered. MEA losses reported herein are only associated with the residue leaving the reclaiming process and do not include losses which may occur elsewhere, such as ammonia formation in the absorber. Further, the VLE of the degraded solvent mixture was predicted by the Aspen Plus thermodynamics model (e-NRTL activity coefficient model coupled with Redlich–Kwong equation of state) due to absence of a relevant VLE model but due to the low composition of the degradation products in the mixture, the employed activity coefficients may not deviate significantly.

We have exemplified the design of the thermal reclamation by using the EfW specifications as case study; different degradation production rates should be expected for the other cases, especially for HSS formation due to for example different oxygen content in the flue gas and absorber temperatures; thermal degradation is expected to be similar across all cases as they all operate at the same pressure and temperature. The differences in the HHS formation will translate to a more intense caustic treatment and adjusting the inventory reclaiming cycle in order not to exceed the 5.74 wt.%. Nevertheless, the trends of MEA, HEEDA and energy recovery should follow similar patterns, and the proposed model can be easily adjusted to different design input specifications. Finally, caustic treatment is assumed to be 100% efficient with stochiometric supply of NaOH and any possible side reactions, such as with CO_2 to make sodium carbonate, are neglected.

Despite these limitations, the current theoretical study is an essential stage in developing PCC and reclaimer configurations and operating condition ranges to be applied in pilot plants (and full-scale operations). The outcomes of this study provide new information on the operational windows of ultra-high capture and different thermal reclaiming options that can inform and be implemented in the long-term (i.e. 12 months or longer) pilot testing on the actual flue gas of interest and with a fully-representative pilot plant, obviously including thermal reclaiming and other solvent management measures such as filters, that is required to give definitive information on a particular real application.

3. Results

3.1 PCC plant

For the CCGT plant, 100% of the added fuel CO_2 corresponds to 99.2% capture of the CO_2 contained in the flue gas. **Figure 4** shows the SRD as a function of the lean loading and the absorber height for zero fossil CO_2 stack operation. When the absorber height increases to 24m from 20m then the SRD drops by ~13% (from 4.42 to 3.84 GJ/tCO_2). Further, the effect of adding intercooling, even if it is not needed to capture the 100% of added fuel CO_2, has been tested for the optimum points in both cases as this can be a preferred operational strategy to limit degradation in the absorber (Mullen, 2024). For the 20m absorber intercooling is applied at 10m (2 beds) and for the 24m at 8m (3 beds). The same intercooling strategy is applied to all cases. For low CO_2 concentrations, such as the CCGT case, intercooling does not appear to offer significant SRD performance gains.

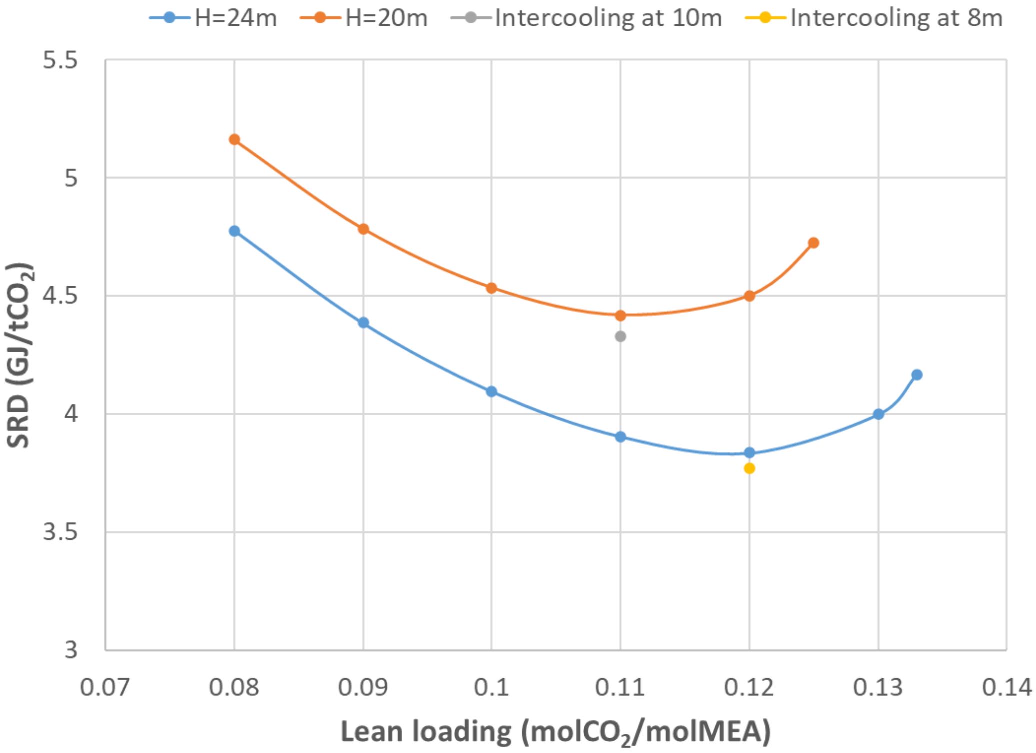

Figure 4. The SRD as function of the lean loading and the absorber height (H) for the CCGT case.

For the cement, FCC and EfW applications, the SRD was, initially, calculated for gross 99% capture of the CO_2 contained in the flue gas and this corresponds to ~99.2-99.4% of the added fuel CO_2 and an absorber height of 20m; for the steel case, due to high CO_2 concentration, the capture fraction is 98.5% (98.7% of the added fuel CO_2). Results in Figure 5 do not include intercooling to showcase that ultra-high capture fractions (gross >98.5%) can be achieved for low lean loadings and slightly increased stripper pressure. As depicted in **Figure 5A**, for a 10m absorber, the optimum SRD in all cases is obtained at a lean loading of 0.10 to 0.12 molCO_2/molMEA and these are 3.50, 3.74, 3.53 and 3.69 GJ/tCO_2 and the calculated L/G ratios are 4.12, 3.34, 2.76 and 1.86 kg/kg for the steel, cement, FCC and EfW plants, respectively. A taller absorber (see **Figure 5B**), 24m, results in reducing the energy penalty of the optimum cases to 3.36, 3.66, 3.42 and 3.49 GJ/tCO_2 and the calculated L/G ratios are 4.01, 3.27, 2.69 and 1.75 kg/kg for the steel, cement, FCC and EfW plants, respectively. It should be noted that based on the simulation results reboiler temperature was not significantly affected by the lean loading and a temperature increase of only around 1K was observed between the 0.08 and 0.13 molCO_2/molMEA loadings for all cases.

The optimum lean loading does not follow the trend of the CO_2 concentration in the flue gas, i.e. 0.12 molCO_2/molMEA for steel (26.4% wet) and EfW (10.1% wet), 0.11 molCO_2/molMEA for FCC (17.7% wet) and 0.1 molCO_2/molMEA for cement (22.5% wet). The CO_2 concentration in the flue gas can affect the optimum lean loading in different ways. Higher CO_2 concentrations can enhance mass transfer but will also result in higher absorber temperatures, as more CO_2 is to be captured (for the same capture fraction), which in turn hinders the absorption of CO_2 (since the latter is exothermic). The maximum temperatures obtained through simulations are 91°C, 89°C, 84°C and 76°C for the steel, cement, FCC and EfW respectively (see table S1 in the Supplementary Information)**.** Hence, it is hard to conclude a concrete correlation between the CO_2 concentration and the optimum lean loading but in any case, this lies between a narrow range for all flues gases (between 0.1 and 0.12 molCO_2/molMEA) and same appeals for the respective SRDs. This illustrates that the proposed design combination of low lean loadings and slightly increased desorber temperature can result in relatively low SRDs and be implemented in all industrial applications.

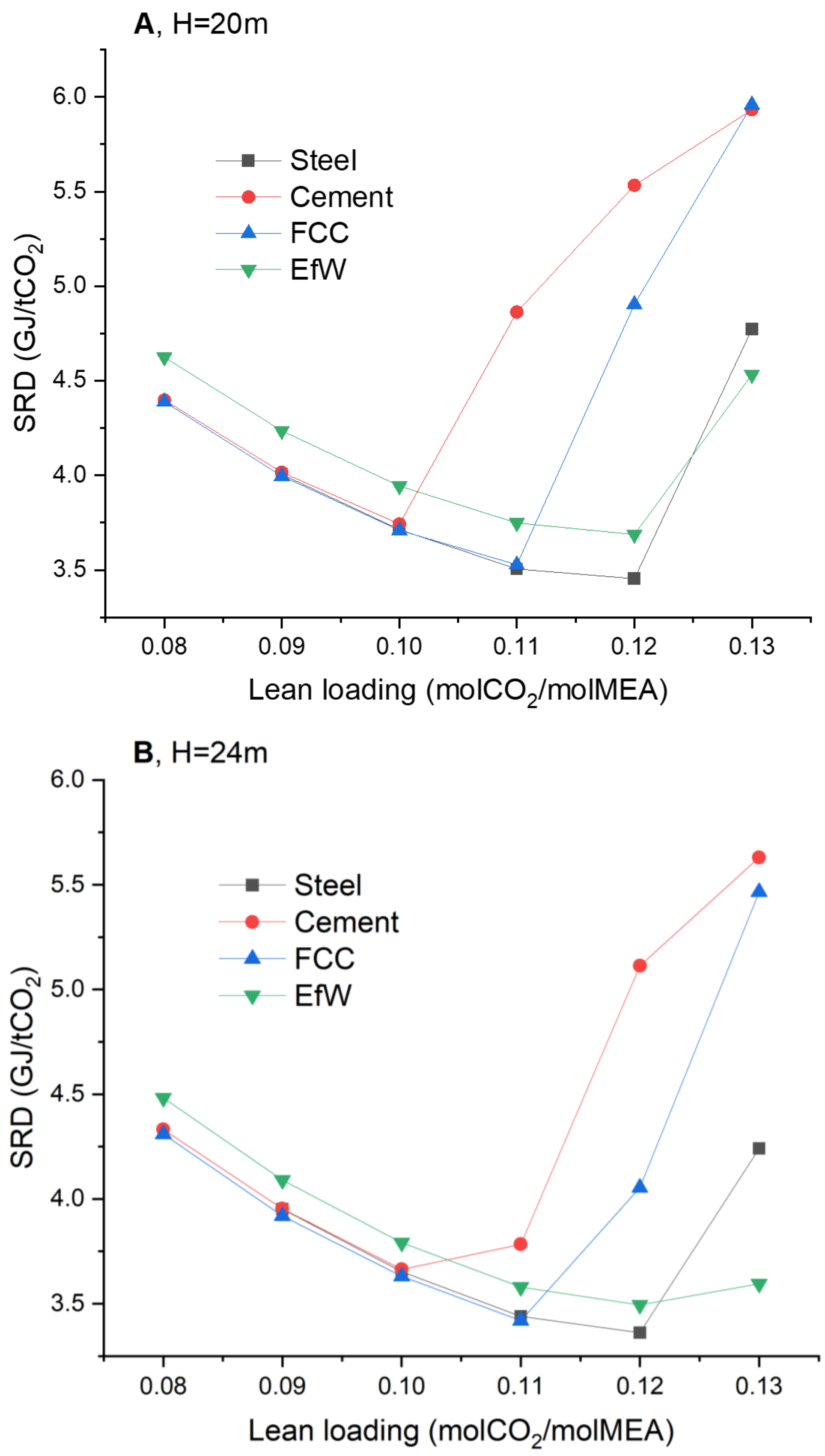

Figure 5. The SRD as function of the lean loading and the absorber height (H) for the steel, cement, FCC and EfW cases. The capture fraction is 99% (for cement, FCC and EfW) and 98.5% (for steel) of the CO_2 contained in the flue gas.

In contrast to the CCGT, zero fossil CO_2 stack operation cannot be achieved without intercooling for the high CO_2 concentration cases; this is due to the high temperatures developed in the absorber since the higher amounts of CO_2 result in releasing more reaction heat, which in turn inhibits mass transfer through the reduction in driving force as the equilibrium CO_2 partial pressure for a given loading rises. As it can been in **Figure 6**, for 99% (98.5% for steel) capture and 20 m absorber, the mass transfer suffers at the top of the absorber for all cases and intercooling helps to shift the equilibrium for better absorber performance.

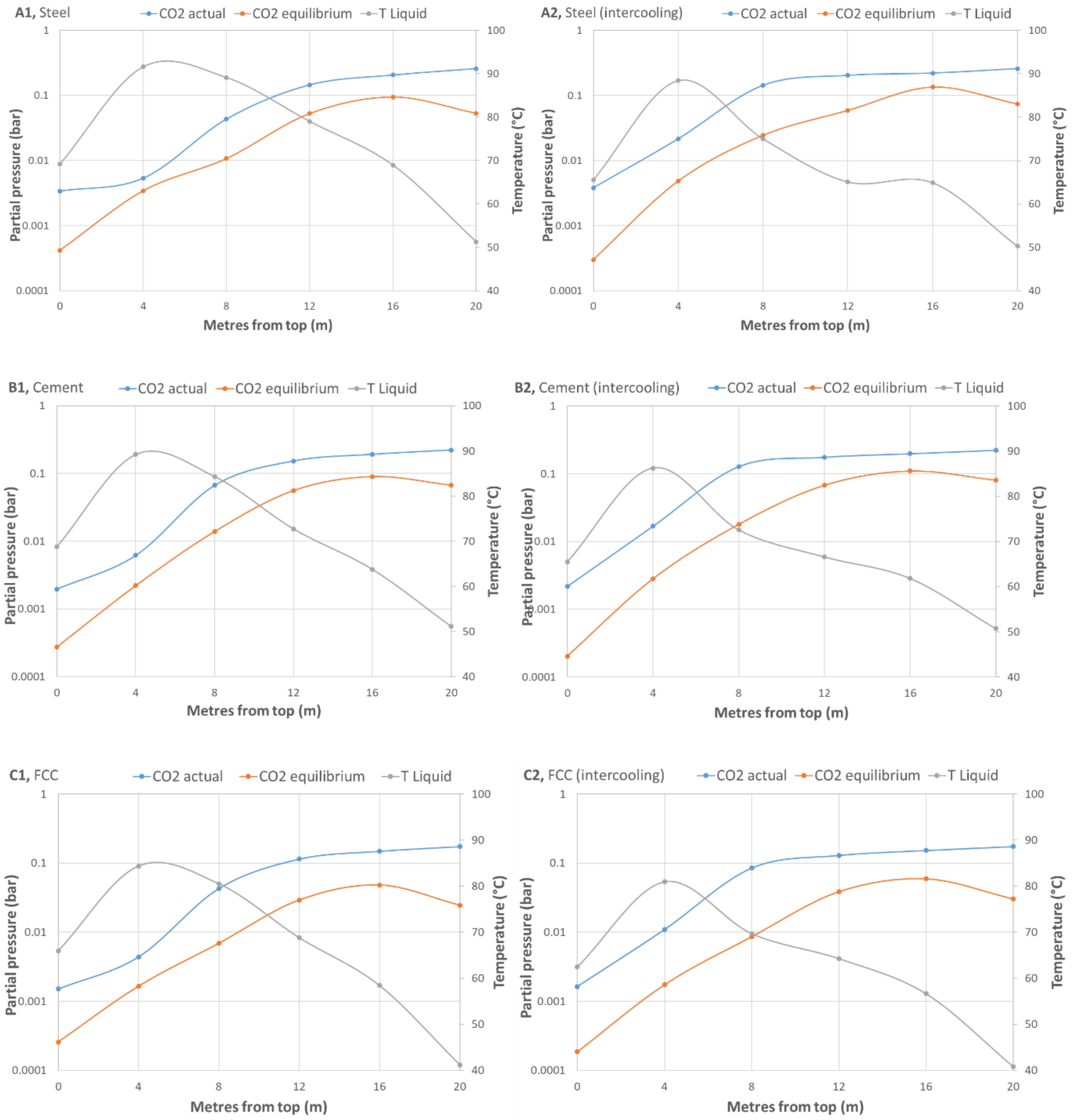

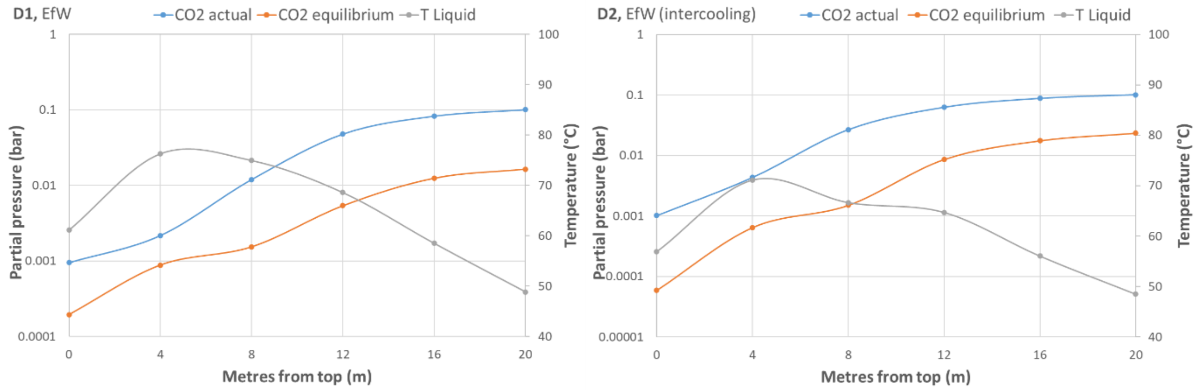

Figure 6. Actual and equilibrium CO_2 partial pressures and temperature profiles along the absorber for 20 m packing height, capture level of 99% (98.5% for steel) and lean loading of 0.10 $molCO_2/molMEA$ for the cement, 0.11 $molCO_2/molMEA$ for the FCC and 0.12 $molCO_2/molMEA$ for the steel and EfW. Intercooling is applied between the 2 beds (10m each) at a temperature of 40°C.

The performance of the absorber is enhanced due to intercooling and higher mass transfer rates are observed at the top of the absorber. Intercooling, however, gave only slightly higher CO_2 loadings at the bottom of the absorber as depicted in **Figure 7A** and this results in an SRD decrease of 1%-1.5%. The same analysis for 24m absorber height, **Figure 7B**, reveals higher rich loadings that in turn lead to lower SRDs compared to the 20m cases.

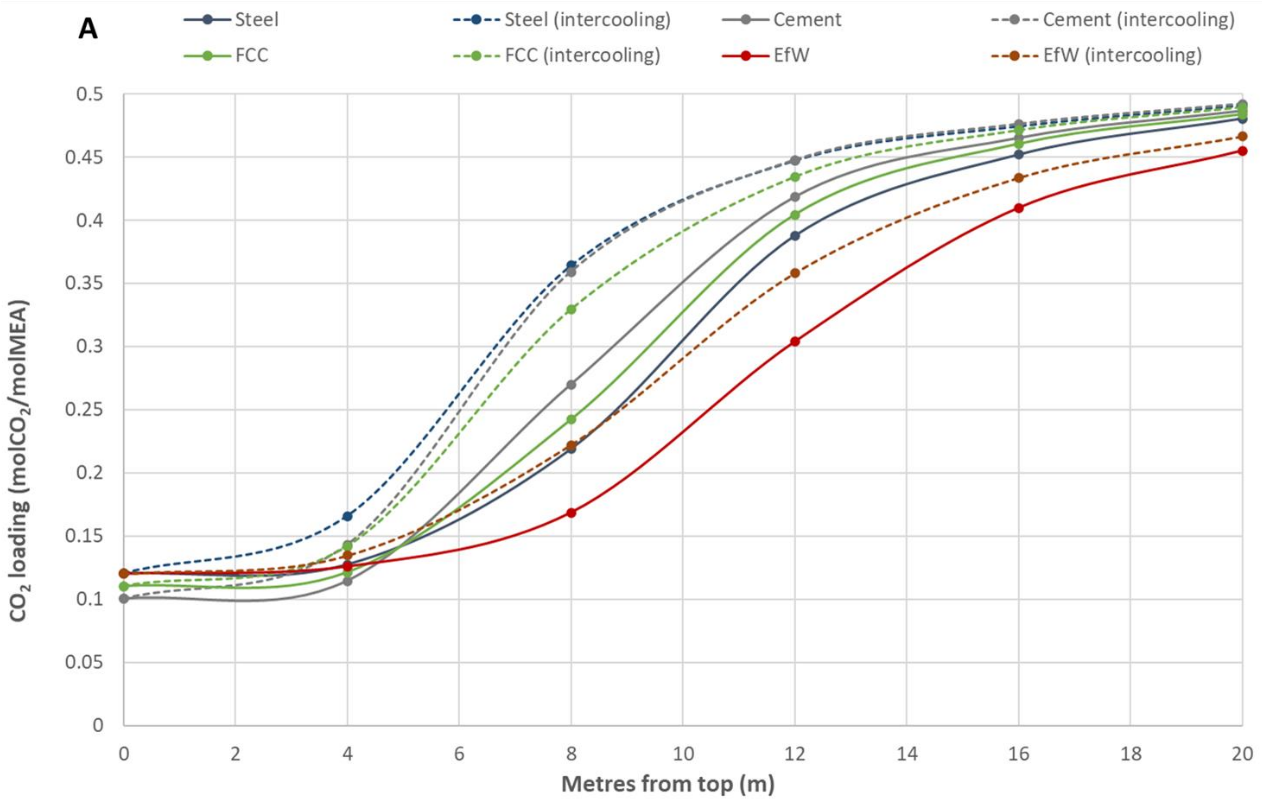

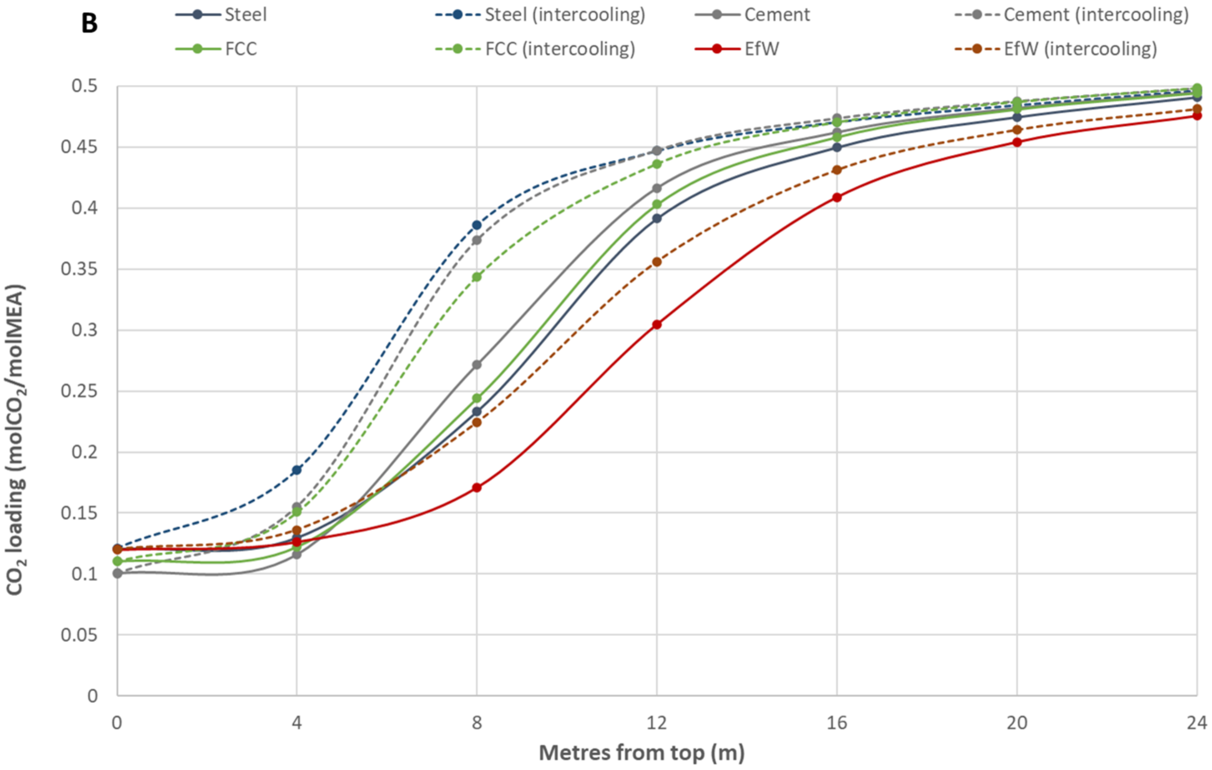

Figure 7. The CO_2 loading evolution along the absorber for 20 m (A) and 24 m (B) packing height and capture level of 99% (98.5% for the steel). Intercooling is applied between the 2 beds (10m each) in A and between the 1st and the 2nd bed in B (3 beds each 8m) at a temperature of 40°C.

Simulations revealed that intercooling is necessary for net-zero capture and that its effect is such that, even without additional packing, 100% of the added fuel CO_2 can be captured in all cases and at moderate SRDs. This is illustrated in **Figure 8** in which the SRD for the steel, cement, FCC and EfW cases at their optimum lean loading is shown for absorber heights of 20m and 24m; intercooling is applied, at 10m for the 20m (2 beds) absorber and at 8m from the top for the 24m absorber (3 beds, between the 1st and the 2nd). For the latter case, the SRD for steel, cement, FCC and EfW is 3.62, 3.96, 3.79 and 3.89 GJ/tCO_2, respectively, and drops to 3.46, 3.75, 3.56 and 3.60 GJ/tCO_2 when the absorber height increases to 24m. These modelling findings therefore also support the idea for extra space in the absorber to allow addition of packing if necessary for high capture designs.

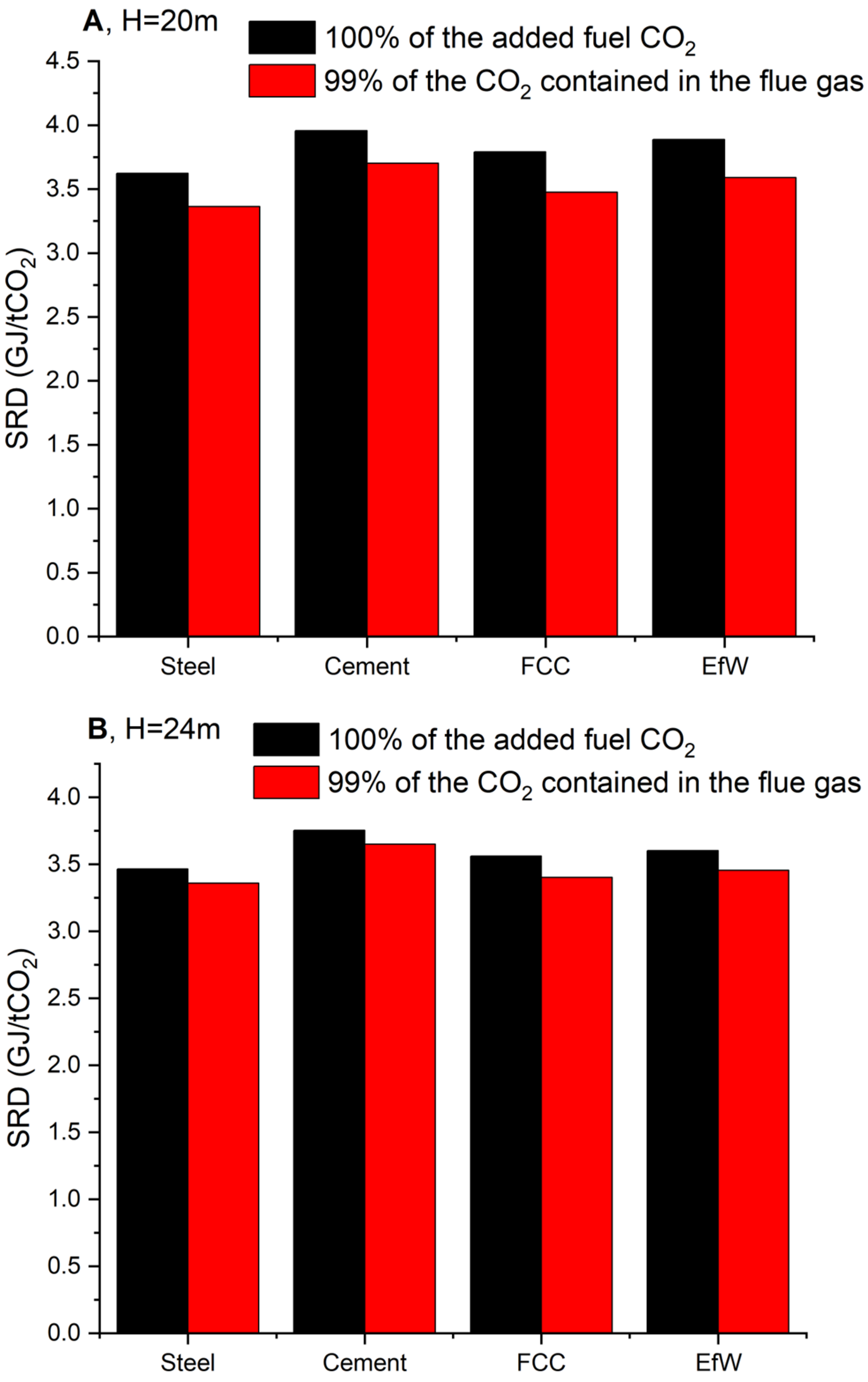

Figure 8. The SRD for different industrial applications for 100% capture of the added fuel CO_2 and 99% capture of the CO_2 contained in the flue gas (~99.2%-99.4% of the added fuel CO_2). Intercooling is applied between the 2 beds (10m each) for the 20m absorber and between the 1st and the 2nd bed

for the 24m (3 beds, 8m each). The lean loading is 0.10 molCO$_2$/molMEA for the cement, 0.11 molCO$_2$/molMEA for the FCC and 0.12 molCO$_2$/molMEA for the steel and EfW.

Table 2 depicts the detailed results for zero fossil CO$_2$ stack operation for each application. The CCGT appears to be kinetically limited at 20m absorber packing height and an increase to 24m of packing provides clear benefits for the energy consumption. But a CCGT will typically operate at reduced load factors, due to the presence of renewable generation in the electricity supply mix, resulting in a CAPEX intensive project and hence only a detailed techno-economic assessment can assess the actual design tradeoffs. Further, the CCGT has low L/G (~1 kg/kg) and this may increase the risk of drying the packing for applications with low CO$_2$ concentrations. It seems likely that this effect has a greater impact for solvents with a CO$_2$ reaction stoichiometry of 1:1 (vs. 2:1 for MEA) if operated at similar L/G ratios. This can be mitigated with the use of specific packing for much lower liquid flows, as in the product literature of Sulzer [30]. The industrial applications will typically operate at high load factors (>85%), making OPEX relatively more important, and hence installation of taller absorbers may make sense from a techno-economic point of view.

Table 2. Results for each case to capture 100% of the added fuel CO_2 (net-zero)

	Flue gas flowrate (kg/s)	%CO_2 (mol, dry)	Absorber diameter (m)		Lean loading ($molCO_2/molMEA$)		Rich loading ($molCO_2/molMEA$)		L/G ratio (kg/kg)		Reboiler duty (MW)		SRD† (GJ/tCO_2)		Intercooling
Absorber height			20m	24m	20m	24m	20m	24m	20m	24m	20m	24m	20m	24m	
CCGT	506.5	5.46	13.5*		0.11	0.12	0.416	0.44	1.05	0.98	342.9	297.7	4.42	3.84	No
Steel	370.2	28.41	14.8		0.12	0.12	0.467	0.485	4.33	4.11	493.0	471.6	3.62	3.46	Yes
Cement	87.2	24.72	7.2		0.10	0.10	0.469	0.489	3.52	3.34	110.0	104.4	3.96	3.75	Yes
FCC	87.2	18.36	7.2		0.11	0.11	0.459	0.482	2.97	2.79	84.2	79.0	3.79	3.56	Yes
EfW	297.8	11.12	11.1		0.12	0.12	0.438	0.465	1.96	1.81	176.7	163.8	3.89	3.6	Yes

**The absorber diameter has been limited to 15m, for the CCGT two identical absorbers working in parallel have been used.*

†the SRDs do not include reclaiming operation

3.2 Operational envelope for PCC

In this section, the authors have analysed the operational window of the PCC design applied in all the investigated applications; it should be noted that no intercooling was considered in this particular practice and that the absorber height is 20m. This analysis provides operational guidelines related to the liquid flow, achieved capture fractions, rich loadings, and SRDs for a fixed lean loading; 0.11 $molCO_2/molMEA$ for all cases apart from cement (0.10 $molCO_2/molMEA$).

Figure 9 provides the operating envelope for each case. As liquid flow in the absorber increases the capture fraction (of the added fuel CO_2) increases until it plateaus to slightly below 100%, indicating again the mass transfer limitations that can only be overcome with intercooling or further reduction of lean loadings [31]. Two critical points for the liquid-to-gas (L/G) ratio exist, both indicated with a dashed black line to identify cases that meet current capture standards (> 95%) and lead to energy efficient operation that is observed for rich loading greater than 0.45 $molCO_2/molMEA$. In the right region, increase of L/G leads to a decrease of the rich loading and in turn this results in increasing the SRD; this showcases the importance of achieving high rich loadings (typically >0.45 $molCO_2/molMEA$). For ultra-high capture fractions, a higher lean-to-rich loading interval – the solvent CO_2 carrying capacity expressed in mol/mol - is necessary for efficient operation. On the other hand, in the left segment of the graphs, low solvent flows restrict capture to lower capture levels than the 95% that is now emerging as standard engineering practice. The optimum flow region can assist in the design of pilot campaigns and operational practice by providing the feasible region of a parameter that can be easily measured and controlled, i.e. the liquid flow.

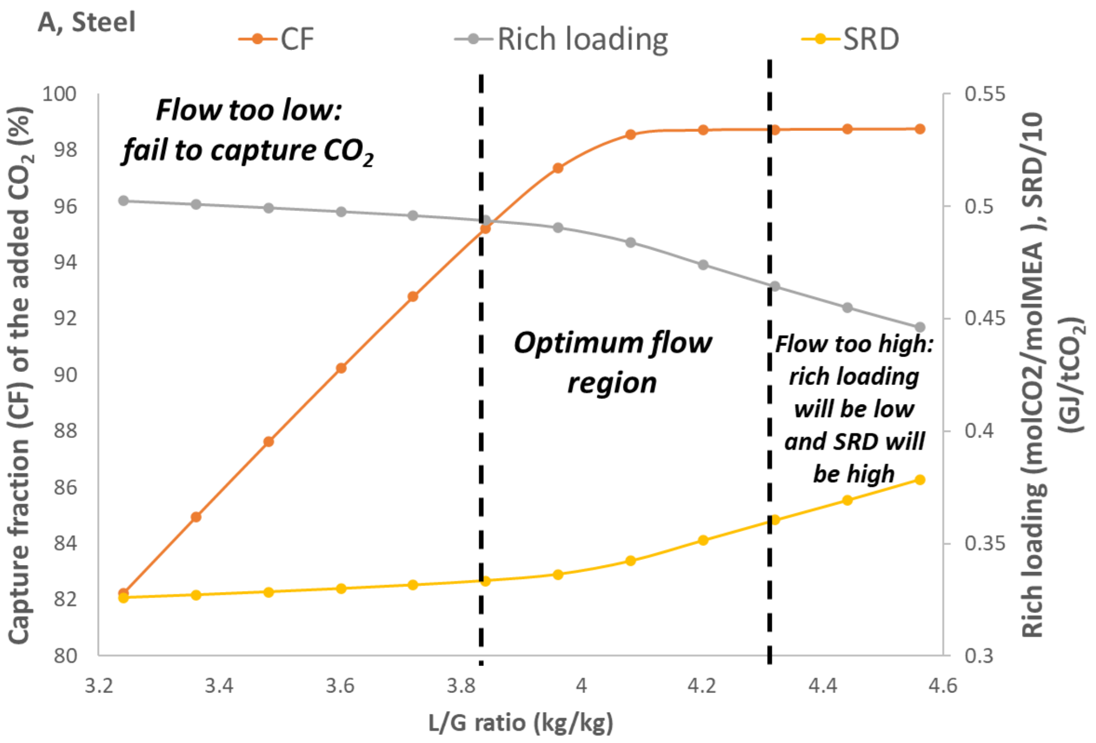
A, Steel
CF
Rich loading
SRD
Flow too low:
fail to capture CO_2
Optimum flow region
Flow too high: rich loading will be low and SRD will be high
Capture fraction (CF) of the added CO_2 (%)
100
98
96
94
92
90
88
86
84
82
80
Rich loading (molCO2/molMEA), SRD/10 (GJ/tCO_2)
0.55
0.5
0.45
0.4
0.35
0.3
3.2
3.4
3.6
3.8
4
4.2
4.4
4.6
L/G ratio (kg/kg)

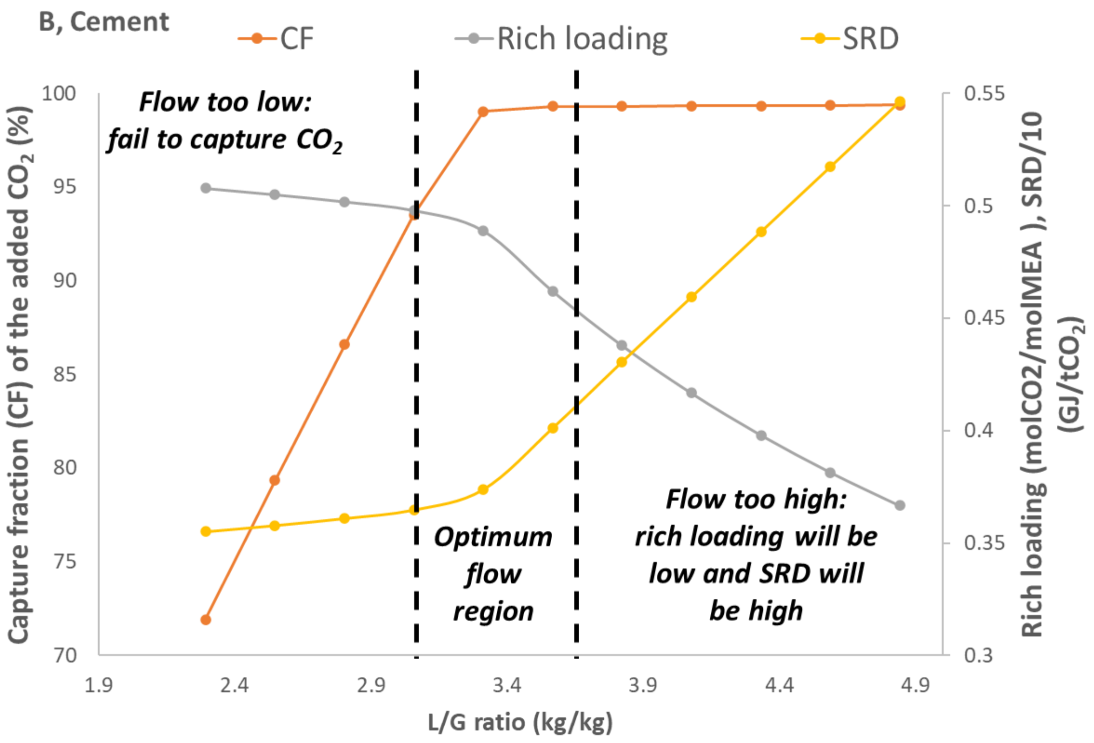
B, Cement
CF
Rich loading
SRD
Flow too low:
fail to capture CO_2
Optimum flow region
Flow too high: rich loading will be low and SRD will be high
Capture fraction (CF) of the added CO_2 (%)
100
95
90
85
80
75
70
Rich loading (molCO2/molMEA), SRD/10 (GJ/tCO_2)
0.55
0.5
0.45
0.4
0.35
0.3
1.9
2.4
2.9
3.4
3.9
4.4
4.9
L/G ratio (kg/kg)

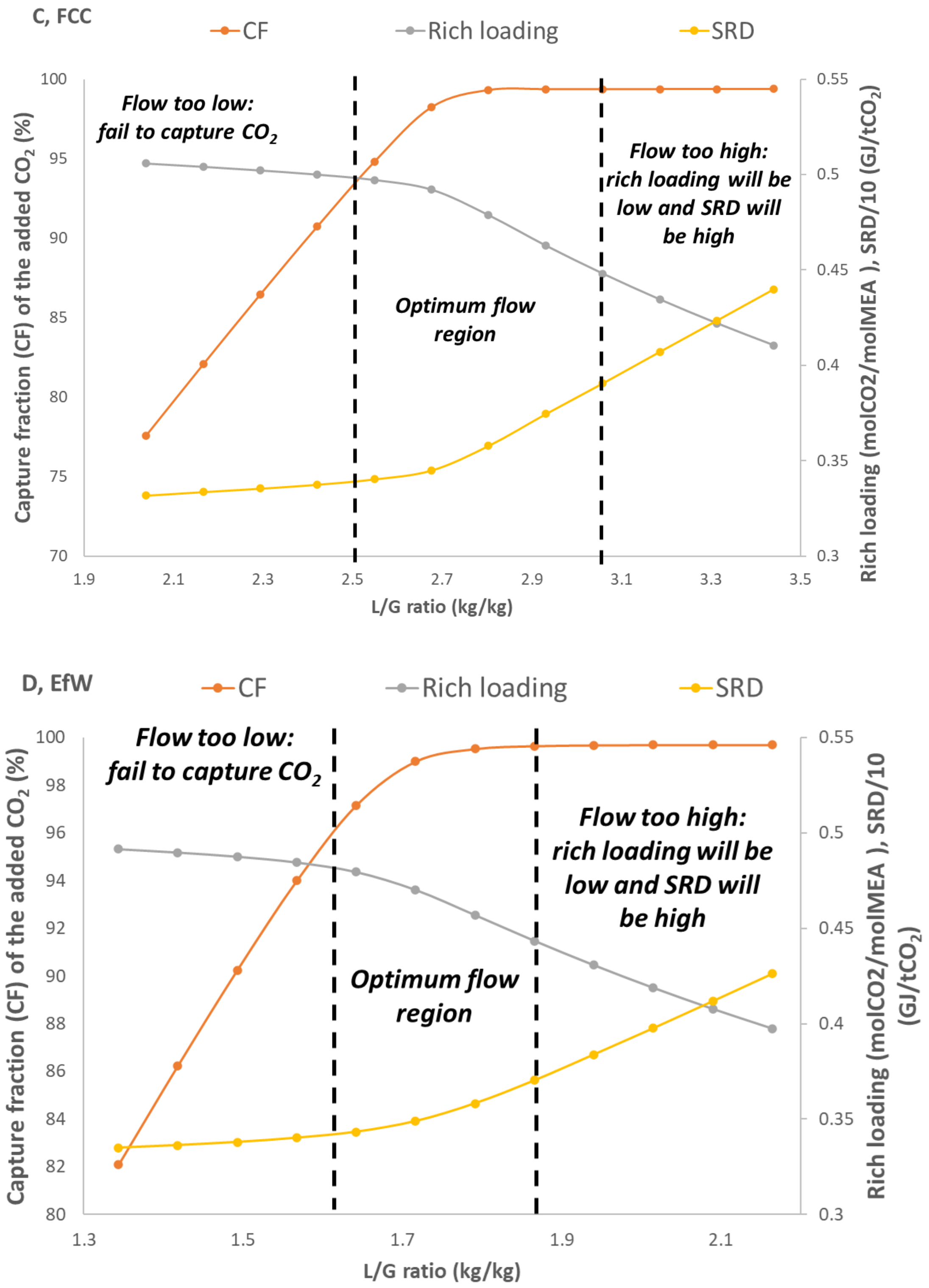

Figure 9. The capture fraction (CF) of the added fuel CO_2, rich loading, and SRD as a function of the liquid-to-gas (L/G) ratio for the EfW case. The lean loading is 0.11 molCO_2/molMEA (0.10 for the cement) and the absorber height is 20m (no intercooling is applied).

3.3 Thermal reclaiming unit

Thermal reclaiming has been considered an energy intensive procedure as it requires evaporation of the solvent at temperatures typically higher than the desorber reboiler. The IEA documented that the energy related to thermal reclaiming is 0.3 GJ/ton CO_2 for a USC PC (ultra supercritical pulverized coal) boiler[32]. In contrast to high boiling point amines, for example DEA and MDEA, MEA can be reclaimed, or partially reclaimed as in this study, at desorber pressures at reclaimer operating temperatures below 150°C to limit thermal degradation.

Results presented in sections 3.1 and 3.2, which considered overall operating patterns for different application, do not include thermal reclaiming, but this will have very limited impact on the presented results. In this section, which is intended specifically to investigate reclaimer operation trends and in particular illustrate trade-offs in operation and the differences between single- and two-stage reclaiming, the PCC EfW plant is integrated with the reclaiming model and as such the vapour stream of the 1st stage is sent to the bottom of the PCC desorber while part of the water derived from the desorber condenser condensate is utilised to enhance MEA stripping. In this study, reclaiming occurs continuously, and it was assumed that caustic treatment to neutralise HSS takes place before the reclaiming; it should be noted that, although caustic treatment has been proposed as an effective practice, more testing is needed to identify the extent of side reactions such as production of sodium carbonate from CO_2. Water is added to assist with MEA stripping, and thus reduce the reclaimer operating temperature required, and this comes from the desorber condenser of the PCC plant.

For 1-stage reclaiming (see **Figure 10A and Table 3**), a temperature of 135°C can recover up to 76% of the MEA but requires high water addition (400% of the reclaimer input). Higher temperatures lead to greater MEA recovery and at lower water additions, e.g. ~88% for a temperature of 140°C and water addition of 300%, and ~91% MEA recovery at 145°C and 200% water addition. In all cases, the whole amount of sodium salts (derived from HSS) is separated from the solvent. On the other hand, the higher the MEA recovery the greater is the amount of HEEDA that is also returned with the solvent and, in the worst case scenario (in terms of HEEDA uptake), ~64% of HEEDA is recycled to the desorber, at 145°C, 400% water addition and MEA recovery of ~97%.

As depicted in **Figure 10B and Table 3**, the 2-stage reclaiming offers a more flexible operational window for high MEA recoveries, >80%, allowing for effective operation at lower temperatures (such as 140°C) if, for example, pilot testing demonstrates significant degradation, and at much lower water inputs, 0%-50% (30%-80% including the water input to the 2nd stage) of the reclaimer feed flow. For example, at 140°C operation, a minimum of 80% MEA recovery at 0% water input (in the 1st reclaimer) can be achieved with an undesirable HEEDA recovery of ~15% and up to ~86% of MEA recovery and ~19% HEEDA recovery when the water input into the 1st reclaimer is increased to 50% of the reclaimer feed. The maximum MEA recovery observed is ~94% accompanied with a maximum undesirable HEEDA uptake at ~32% at a temperature of 145°C and 50% water input in the 1st reclaimer. In all cases, as would be expected, the whole amount of non-volatile components (sodium salts) are removed. In the 2-stage configuration, most of the HEEDA that is returned to the PCC solvent inventory is carried over from the 2nd stage, reporting in the 'to amine tank stream' as labelled in Figure 3. The MEA concentration in the amine tank is between 26%-33% wt. (unloaded) while HEEDA is present at 0.33%-1.4% wt%. concentrations and this level of HEEDA (as a proxy for all volatile degradation products) is still expected to be a satisfactory solvent composition. Indeed, while the reaction chemistry of such blends can be complex and hard to model, Jorgensen et al. [33] concluded that *'In the presence of MEA, HEEDA and MEA can act like a solvent blend, resulting in multiple carbamates forming within the solven*t' indicating that impurities such as HEEDA may not significantly affect the CO_2 carrying capacity.

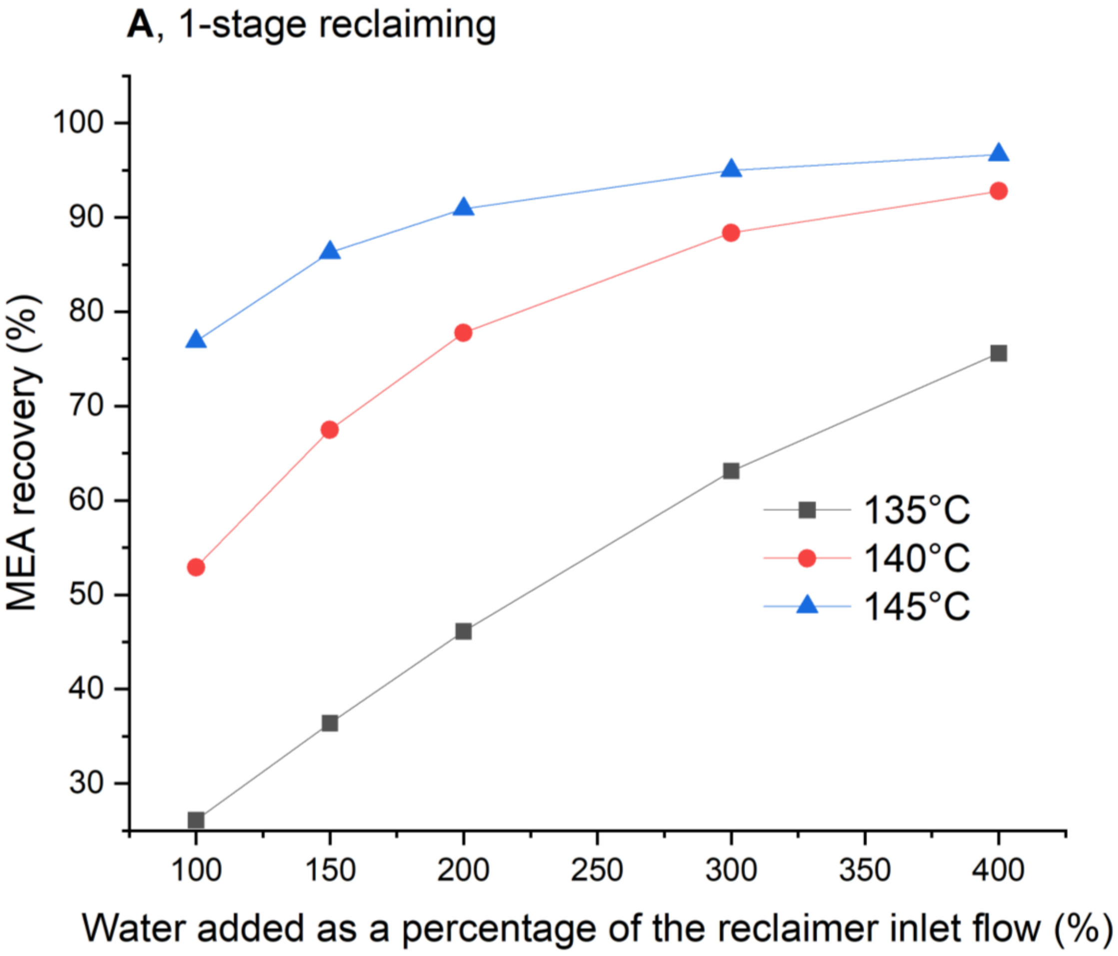

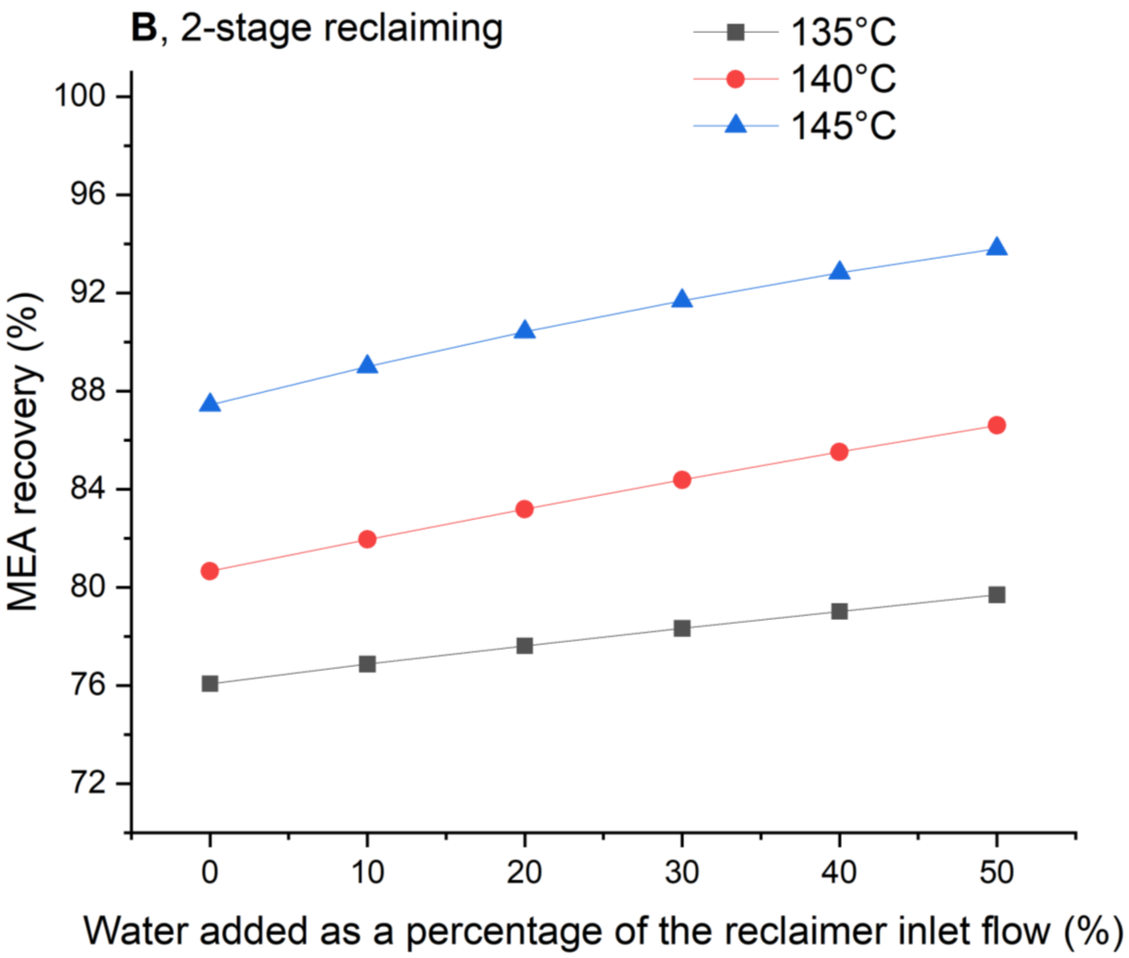

Figure 10. The MEA recovery as a function of the water added in the 1st reclaimer. Water at the 2nd reclaimer is fixed at 30% of the inlet flow. Both stages operate at the same temperature.

In all cases, the higher the solvent recovery, the greater the HEEDA recovery. Long term pilot testing should optimise the trade-off between solvent recovery and degradation uptake but obviously in any case fresh solvent addition will be necessary and therefore a low-cost solvent, such as MEA, can be beneficial for cost-effective operations. Table 3 summarises the recovery fractions of HEEDA and MEA for all the thermal reclaiming scenarios investigated herein. The 2-stage configuration operating at 145°C appears to be a preferred solution as it can recover more than 87% up to 94% of the MEA and limit the HEEDA recovery between 23%-31%.

The accurate impact, i.e. additional degradation, of operating the reclaimer at elevated temperatures of up to 145°C - compared to operation at 135°C – cannot, however, be quantified in this study -only extended pilot testing under fully-realistic conditions would be able to do so. Although a 10°C increase is expected to increase the rate of thermal degradation of MEA by a factor of two, this would be mitigated by a reduction of the concentration of thermally degrading carbamate ions due to low lean loading operation at 0.1 $molCO_2/molMEA$. For example, Mullen and Lucquiaud [10] predicted that thermal degradation at 145°C and 0.06 $molCO_2/molMEA$ increases by a factor of 1.65

compared to thermal degradation at 135°C and 0.1 molCO$_2$/molMEA. Further action towards mitigation of thermal degradation could also be achieved by designing and engineering the reclaimer stages to minimise the residence time of the amine before evaporation.

Table 3. Summary of the thermal reclaiming results

Reclaiming temperature	135°C		140°C		145°C	
	HEEDA recovery (%)	MEA recovery (%)	HEEDA recovery (%)	MEA recovery (%)	HEEDA Recovery (%)	MEA recovery (%)
Water added*	**1-stage reclaiming**					
100%	1.84	26.12	5.30	52.92	14.21	76.89
150%	2.85	36.39	9.23	67.49	24.73	86.27
200%	4.13	46.12	14.68	77.77	35.33	90.89
300%	7.77	63.11	27.94	88.37	52.42	94.97
400%	13.17	75.58	40.52	92.78	63.78	96.67
Water added*	**2-stage reclaiming**					
0%	11.39	76.07	15.25	80.66	23.34	87.43
10%	11.71	76.87	15.94	81.95	24.88	88.99
20%	12.01	77.62	16.66	83.19	26.51	90.41
30%	12.30	78.33	17.41	84.38	28.22	91.68
40%	12.59	79.02	18.19	85.51	30.01	92.81
50%	12.87	79.69	19.02	86.60	31.86	93.81
**water added in the 1st reclaimer as a percentage of the reclaimer input mass flowrate. For the 2-stage configuration a fixed amount of water, equal to 30% of the reclaimer feed, is added in all cases.*						

Figure 11 presents the additional energy penalty incurred due to reclaiming as a percentage of the desorber reboiler duty of the standalone PCC plant. As heat is recovered only in the 1st reclaimer, the 1-stage configuration is associated with lower energy penalties than the 2-stage reclaiming arrangements. For single stage, an approximately linear relation exists for all cases between the additional thermal energy and the operating temperature and the difference between cases operating at same water input is too small for the thermal energy penalty to be a decisive design parameter. For the 2-stage configuration there is a small amount of noise in the results, but the differences can be considered insignificant, and it can be seen that for 135°C, 140°C and 145°C the additional thermal energy duty is approximately 0.6%, 0.5% and 0.4% of the desorber duty, respectively. Considering both reclaiming cases the thermal energy penalty ranges between 0.004 and 0.024 GJ/tonne of CO_2 captured.

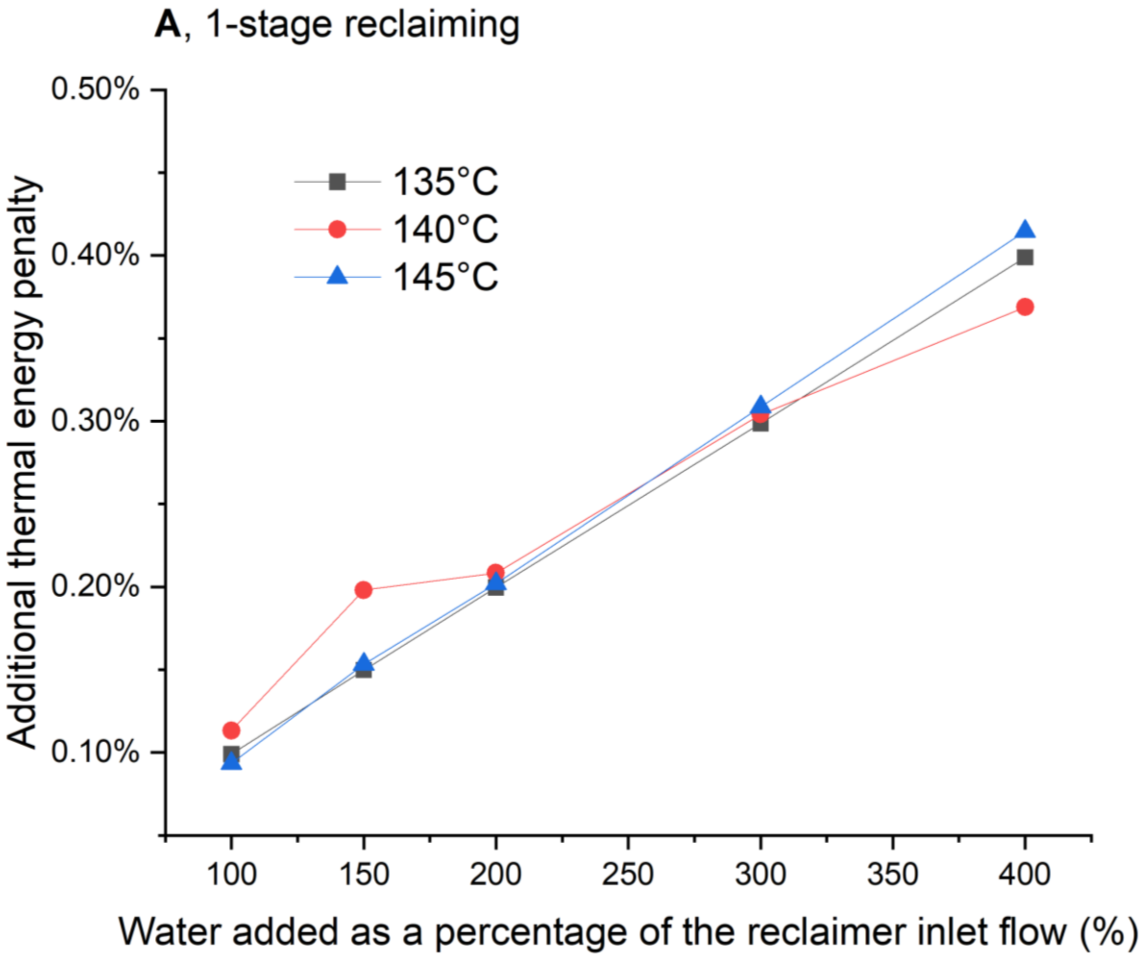

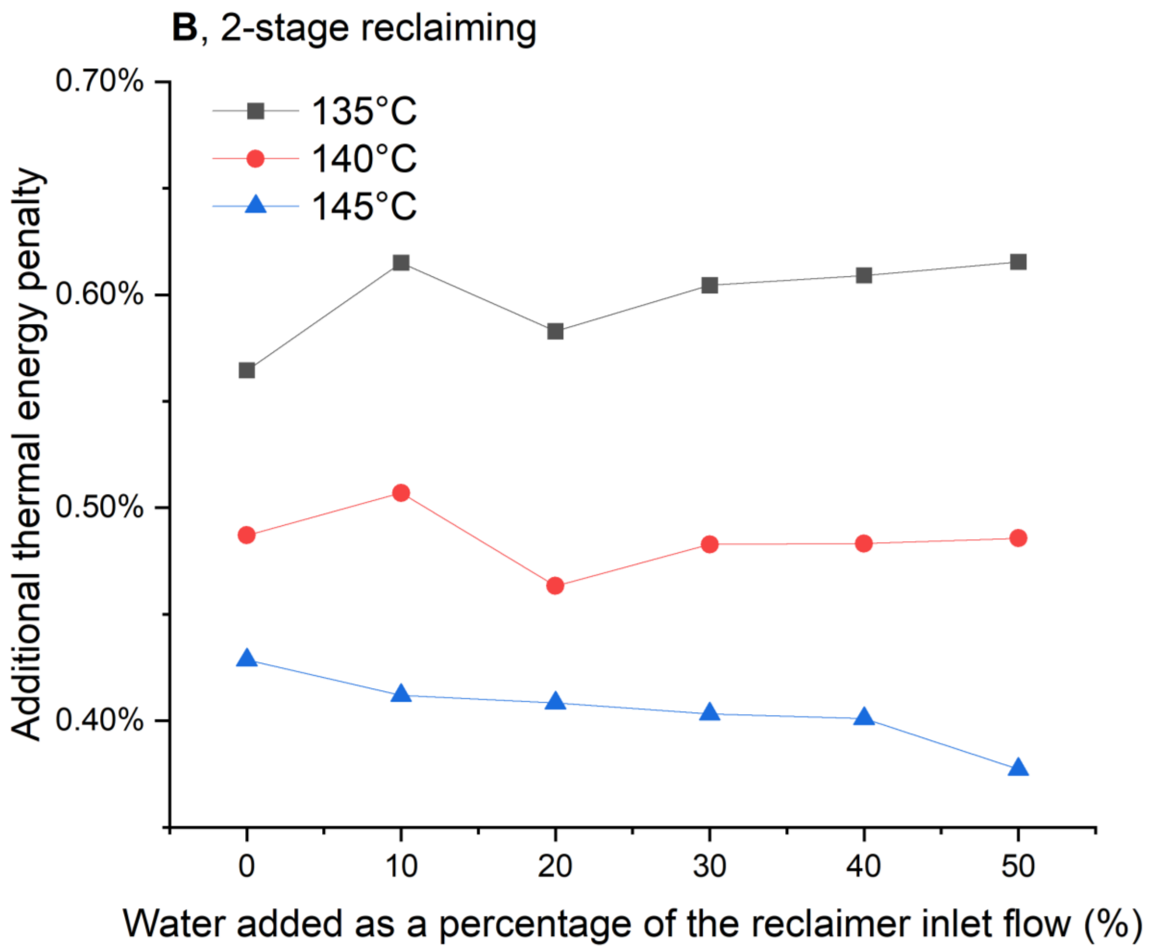

Figure 11. The additional thermal energy penalty due to reclaiming expressed in % of the desorber reboiler duty (=176.7 MWth) as a function of the water added, A) 1-stage reclaiming, B) 2-stage reclaiming.

3.4 Electricity lost

As reclaiming operates at higher temperatures than the desorber, steam of higher quality is required to provide the necessary heat load. Heat for the reclaimer is assumed to be provided by steam at 152°C, 5 bar (extracted at 6 bar) while for the desorber reboiler LP steam of 135°C, 3.15 bar (extracted at 3.5 bar) is used. The aim of this section is to calculate the energy used for the thermal reclaiming. The methodology used is based on that presented in [5]. The steam extracted from the steam turbine cycle results in a reduction in the power produced in that cycle.

Figure 12 is the Mollier (enthalpy-entropy) diagram presenting the steam extraction and inlet states to the PCC for both the reboiler and the reclaimer units as well as the approximate steam turbine expansion line. The calculated electricity output lost per unit heat supplied is 0.277 MJe/MJth for the reclaimer and 0.234 MJe/MJth for the desorber (calculations can be found in the Supplementary Information).

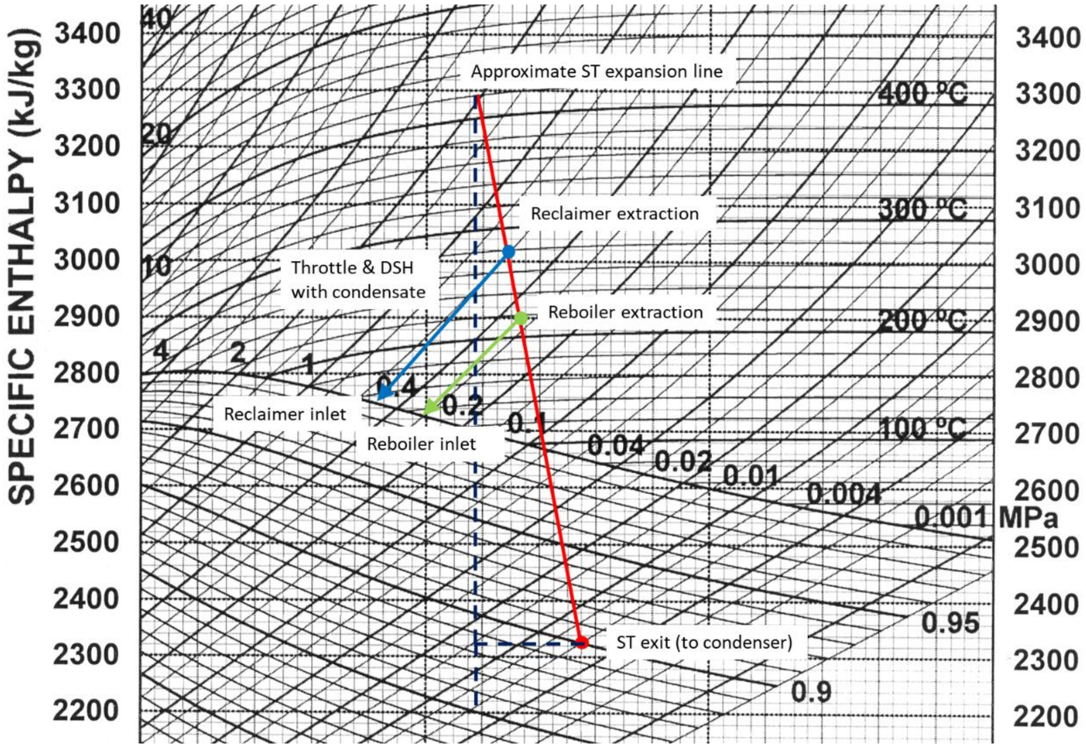

Figure 12. Mollier Diagram for Water-Steam with steam extraction points for the reboiler of the desorber and the reclaimer (Gibbins and Lucquiaud, 2024)

Figure 13 shows the % increase of the equivalent electricity lost due to the addition of reclaiming from the electricity lost in the desorber reboiler duty; electricity loss of the PCC plant without reclaiming has been calculated as ~41.35 MWe for the EfW case –. The heat integration of the reclaiming with the PCC desorber limits the additional electricity lost to ~1.13%, relative to the case that no reclaiming is employed, for the most energy intensive case (~41.82 MWe) i.e., 1-stage, 400% water addition and 145°C (MEA recovery is ~94%). This small increase shows that energy costs for MEA reclaiming do not constitute a serious obstacle.

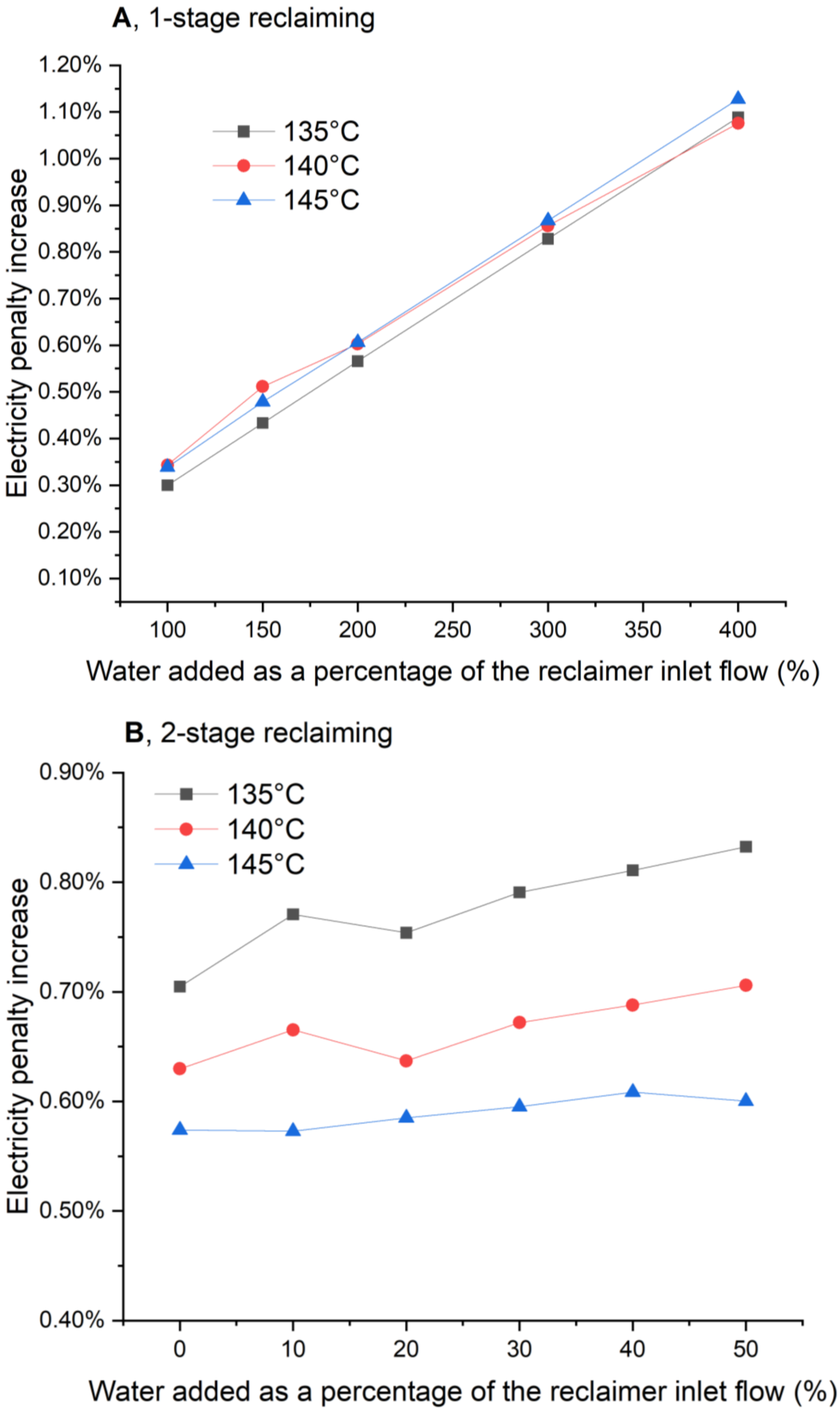

Figure 13. The %increase of the equivalent electricity lost, due to thermal solvent reclaiming, from the electricity lost in the desorber reboiler without reclaiming for A) 1-stage reclaiming and B) 2-stage reclaiming for the EfW operating case. Equivalent electricity lost due to desorber reboiler duty is 41.35 MWe without reclaiming.

4. Conclusions

The research is a first of a kind study in presenting a modelling assessment of coupling PCC to a number of applications including power generation, CCGT, and industrial applications steel, cement, EfW and FCC aiming at ultra-high capture fractions and zero fossil CO_2 stack operation. In addition, we have modelled and analysed for the first time various designs of integrating continuous solvent thermal reclaiming to the PCC plant based on data from pilot studies.

It was found that, by operating at low lean loadings and a desorber pressure of 2.4 bar, equivalent net zero fossil CO_2 stack emissions can be achieved with SRDs lower than 4GJ/tCO_2; for the industrial applications, i.e. steel, cement, EfW and FCC, intercooling is required to capture 100% of the added fuel CO_2, due to the relatively high CO_2 content in the flue gas. For an absorber packing height of 20m (industrial two-bed standard) the optimum lean loading is 0.1-0.12 molCO_2/molMEA. A taller absorber can reduce the energy penalty, but the resulted CAPEX vs OPEX trade-off should be thoroughly investigated. The SRD for steel, cement, FCC and EfW is 3.62, 3.96, 3.79 and 3.89 GJ/tCO_2, respectively, and drops to 3.46, 3.75, 3.56 and 3.60 GJ/tCO_2 when the absorber height increases to 24m (three-bed standard).

Further, two designs for thermal reclaiming have been analysed, i.e. 1- and 2-stage, and modelled using both volatile and non-volatile illustrative typical components. These reclaimer designs can recover up to ~97% of the neutralised MEA that undergoes reclaiming. The modelling assumes that Heat Stable Salts are converted to sodium salts (non-volatile compounds) and as such they are completely removed. Nevertheless, high MEA recoveries will lead to increased recycling of the volatile thermal degradation products too and hence higher equilibrium concentrations in the solvent inventory in order to balance rates of impurity production with rates of removal. To analyse this results are presented for a wide range of operating parameters and these suggest that for the 2-stage reclaiming operating at 145°C, MEA recovery of 87% up to 94% of will only recycle between 23%-32% of thermal degradation products, using HEEDA as a proxy (as the most volatile major component) for all volatile thermal degradation products. The 1-stage reclaiming can offer a simpler design and achieve an MEA recovery of ~91% with an unwanted HEEDA recycle rate of ~35% for 145°C operation but it comes with water consumption that may affect the absorber/desorber water balance negatively. Further, the integration of the reclaimer with the PCC results in a small additional electricity penalty of up to 1.13% relative to the desorber equivalent electricity reboiler duty when no reclaiming is considered. Overall, the analysed reclaiming designs are suggested as useful representations of the options available for sustained PCC operation with full thermal reclaiming.

The research provides for the first time trends and guidelines for operation at ultra-high capture fractions and effective solvent reclaiming. As actual capture rates depend on both capture fractions and plant availability, the study provided useful operational guidelines to industrial application (typically operated at capacity factors of >85%) in order to assist in the successful deployment of PCC plants. This modelling study can also inform further research, in particular future projects aiming to demonstrate pilot-testing and commercial operation of ultra-high capture for deep removal PCC with thermal reclaiming.

Acknowledgments

We would like to acknowledge that this work was supported by the UKRI ISCF Industrial Decarbonisation Challenge, through the UK Industrial Decarbonisation Research and Innovation Centre (IDRIC) award number: EP/V027050/1, under the Industrial Decarbonisation Challenge (IDC). Further, the authors would like to acknowledge the Engineering and Physical Sciences Research Council (EPSRC) under the United Kingdom CCS Research Centre grant EP/W002841/1.

Supporting Information: Additional methods for calculating solvent inventory, reclaiming material balances and heat to electricity conversion efficiency.

References

---

(1) GOV.UK. *Government reignites industrial heartlands 10 days out from the International Investment Summit*. 2024. https://www.gov.uk/government/news/government-reignites-industrial-heartlands-10-days-out-from-the-international-investment-summit (accessed.
(2) Mitsubishi. *MHI Selected as Licensor of CO2 Capture Technology for Leading Low Carbon Hydrogen Production Project in Cheshire, UK*. 2024. https://www.mhi.com/news/24031201.html (accessed.
(3) Brandl, P.; Bui, M.; Hallett, J. P.; Mac Dowell, N. Beyond 90% capture: Possible, but at what cost? *International Journal of Greenhouse Gas Control* **2021**, *105*, 103239. DOI: https://doi.org/10.1016/j.ijggc.2020.103239.
(4) EA. *Guidance: Post-combustion Carbon Dioxide Capture: Best Available Techniques (BAT)*. 2021. https://www.gov.uk/guidance/post-combustion-carbon-dioxide-capture-best-available-techniques-bat (accessed.
(5) Gibbins, J.; Lucquiaud, M. *BAT Review for New-Build and Retrofit PostCombustion Carbon Dioxide Capture Using Amine-Based Technologies for Power and CHP Plants Fuelled by Gas and Biomass as an Emerging Technology under the IED for the UK. UKCCSRC Report.*; 2021. https://ukccsrc.ac.uk/best-available-technology-bat-information-for-ccs/.
(6) Hirata, T.; Tsujiuchi, T.; Kamijo, T.; Kishimoto, S.; Inui, M.; Kawasaki, S.; Lin, Y.-J.; Nakagami, Y.; Nojo, T. Near-zero emission coal-fired power plant using advanced KM CDR process™. *International Journal of Greenhouse Gas Control* **2020**, *92*, 102847. DOI: https://doi.org/10.1016/j.ijggc.2019.102847.
(7) Feron, P.; Cousins, A.; Jiang, K.; Zhai, R.; Shwe Hla, S.; Thiruvenkatachari, R.; Burnard, K. Towards Zero Emissions from Fossil Fuel Power Stations. *International Journal of Greenhouse Gas Control* **2019**, *87*, 188-202. DOI: https://doi.org/10.1016/j.ijggc.2019.05.018. Shah, M. I.; Silva, E.; Gjernes, E.; Åsen, K. I. Cost Reduction Study for MEA based CCGT Post-Combustion CO 2 Capture at Technology Center Mongstad. In 15th Greenhouse Gas Control Technologies Conference 15-18 March 2021, Abu Dhabi; 2021.
(8) Du, Y.; Gao, T.; Rochelle, G. T.; Bhown, A. S. Zero- and negative-emissions fossil-fired power plants using CO2 capture by conventional aqueous amines. *International Journal of Greenhouse Gas Control* **2021**, *111*, 103473. DOI: https://doi.org/10.1016/j.ijggc.2021.103473.

(9) Michailos, S.; Gibbins, J. A Modelling Study of Post-Combustion Capture Plant Process Conditions to Facilitate 95–99% CO2 Capture Levels From Gas Turbine Flue Gases. *Frontiers in Energy Research* **2022**, *10*, Original Research. DOI: 10.3389/fenrg.2022.866838.
(10) Mullen, D.; Lucquiaud, M. On the Cost of Zero Carbon Electricity: A Techno-Economic Analysis of Combined Cycle Gas Turbines with Post-Combustion CO2 Capture. **2024**.
(11) Endo, T.; Kajiya, Y.; Nagayasu, H.; Iijima, M.; Ohishi, T.; Tanaka, H.; Mitchell, R. Current status of MHI CO2 capture plant technology, large scale demonstration project and road map to commercialization for coal fired flue gas application. *Energy Procedia* **2011**, *4*, 1513-1519. DOI: https://doi.org/10.1016/j.egypro.2011.02.019.
(12) Hirata, T.; Nagayasu, H.; Yonekawa, T.; Inui, M.; Kamijo, T.; Kubota, Y.; Tsujiuchi, T.; Shimada, D.; Wall, T.; Thomas, J. Current Status of MHI CO2 Capture Plant technology, 500 TPD CCS Demonstration of Test Results and Reliable Technologies Applied to Coal Fired Flue Gas. *Energy Procedia* **2014**, *63*, 6120-6128. DOI: https://doi.org/10.1016/j.egypro.2014.11.644.
(13) Radgen, P.; Rode, H.; Reddy, S.; Yonkoski, J. Lessons Learned from the Operation of a 70 Tonne per Day Post Combustion Pilot Plant at the Coal Fired Power Plant in Wilhelmshaven, Germany. *Energy Procedia* **2014**, *63*, 1585-1594. DOI: https://doi.org/10.1016/j.egypro.2014.11.168. Reddy, S.; Scherffius, J. R.; Yonkoski, J.; Radgen, P.; Rode, H. Initial Results from Fluor's CO2 Capture Demonstration Plant Using Econamine FG PlusSM Technology at E.ON Kraftwerke's Wilhelmshaven Power Plant. *Energy Procedia* **2013**, *37*, 6216-6225. DOI: https://doi.org/10.1016/j.egypro.2013.06.550. Reddy, S.; Yonkoski, J.; Rode, H.; Irons, R.; Albrecht, W. Fluor's Econamine FG PlusSM Completes Test Program at Uniper's Wilhelmshaven Coal Power Plant. *Energy Procedia* **2017**, *114*, 5816-5825. DOI: https://doi.org/10.1016/j.egypro.2017.03.1719.
(14) NCCC. *Testing of Hitachi H3-1 Solvent at the National Carbon Capture Center:*

Final Report; 2016. https://www.nationalcarboncapturecenter.com/wp-content/uploads/2021/01/Hitachi-Power-Systems-America-Testing-of-Hitachi-H3-1-Solvent-2012.pdf.
(15) Garg, B.; Haque, N.; Cousins, A.; Pearson, P.; Verheyen, T. V.; Feron, P. H. M. Techno-economic evaluation of amine-reclamation technologies and combined CO2/SO2 capture for Australian coal-fired plants. *International Journal of Greenhouse Gas Control* **2020**, *98*, 103065. DOI: https://doi.org/10.1016/j.ijggc.2020.103065.
(16) Putta, K. R.; Saldana, D.; Campbell, M.; Shah, M. I. Development of CO_2 capture process cost baseline for 555 MWe NGCC power plant using standard MEA solution. In Proceedings of the 16th Greenhouse Gas Control Technologies Conference (GHGT-16) 23-24 Oct 2022, 2022.
(17) CCSI. *CCSI Toolset: MEA Steady State Model*. 2021. https://github.com/CCSI-Toolset/ (accessed.
(18) Elliott, W.; Benz, A.; Gibbins, J.; Michailos, S. An open-access FEED study for a post-combustion CO2 capture plant retrofit to a CCGT. In Proceedings of the 16th Greenhouse Gas Control Technologies Conference (GHGT-16) 23-24 Oct 2022, 2022. Elliott, W.; Benz, A.; Gibbins, J.; Michailos, S. An Open-Access, Detailed Description of Post-Combustion CO2 Capture Plant. In *Proceedings of the 16th Greenhouse Gas Control Technologies Conference (GHGT-16) 23-24 Oct 2022*, 2022.
(19) Elliot, W. *Front-End Engineering Design (FEED) Study for a Carbon Capture Plant Retrofit to a Natural Gas-Fired Gas Turbine Combined Cycle Power Plant (2x2x1 Duct-Fired 758-MWe Facility with F Class Turbines)*; 2021. https://www.osti.gov/biblio/1836563.
(20) Flø, N. E.; Faramarzi, L.; de Cazenove, T.; Hvidsten, O. A.; Morken, A. K.; Hamborg, E. S.; Vernstad, K.; Watson, G.; Pedersen, S.; Cents, T.; et al. Results from MEA Degradation and Reclaiming Processes at the CO2 Technology Centre Mongstad. *Energy Procedia* **2017**, *114*, 1307-1324. DOI: https://doi.org/10.1016/j.egypro.2017.03.1899. Morken, A. K.; Pedersen, S.; Kleppe, E. R.; Wisthaler, A.; Vernstad, K.; Ullestad, Ø.; Flø, N. E.; Faramarzi, L.; Hamborg, E. S. Degradation and Emission Results of Amine Plant Operations from MEA Testing at the CO2 Technology Centre Mongstad. *Energy Procedia* **2017**, *114*, 1245-1262. DOI: https://doi.org/10.1016/j.egypro.2017.03.1379.
(21) Faramarzi, L.; Thimsen, D.; Hume, S.; Maxon, A.; Watson, G.; Pedersen, S.; Gjernes, E.; Fostås, B. F.; Lombardo, G.; Cents, T.; et al. Results from MEA Testing at the CO2 Technology Centre Mongstad:

Verification of Baseline Results in 2015. *Energy Procedia* **2017**, *114*, 1128-1145. DOI: https://doi.org/10.1016/j.egypro.2017.03.1271.

(22) Mullen, D.; Braakhuis, L.; Knuutila, H. K.; Gibbins, J.; Lucquiaud, M. Monoethanolamine Degradation Rates in Post-combustion CO2 Capture Plants with the Capture of 100% of the Added CO2. *Industrial & Engineering Chemistry Research* **2024**, *63* (31), 13677-13691. DOI: 10.1021/acs.iecr.4c01525.

(23) Braakhuis, L.; Knuutila, H. K. Predicting solvent degradation in absorption–based CO2 capture from industrial flue gases. *Chemical Engineering Science* **2023**, *279*, 118940. DOI: https://doi.org/10.1016/j.ces.2023.118940.

(24) Braakhuis, L.; Høisæter, K. K.; Knuutila, H. K. Modeling the Formation of Degradation Compounds during Thermal Degradation of MEA. *Industrial & Engineering Chemistry Research* **2022**, *61* (7), 2867-2881. DOI: 10.1021/acs.iecr.1c04496.

(25) IEAGHG. *Gaseous Emissions from Amine Based Post-combustion CO2. Capture Processes and Their Deep Removal. Report 2012/07.*; 2012. Zoannou, K.-S.; Sapsford, D. J.; Griffiths, A. J. Thermal degradation of monoethanolamine and its effect on CO2 capture capacity. *International Journal of Greenhouse Gas Control* **2013**, *17*, 423-430. DOI: https://doi.org/10.1016/j.ijggc.2013.05.026.

(26) ChemSpider. *Search and share chemistry*. https://www.chemspider.com/ (accessed.

(27) Roussanaly, S.; Fu, C.; Voldsund, M.; Anantharaman, R.; Spinelli, M.; Romano, M. Techno-economic Analysis of MEA CO2 Capture from a Cement Kiln – Impact of Steam Supply Scenario. *Energy Procedia* **2017**, *114*, 6229-6239. DOI: https://doi.org/10.1016/j.egypro.2017.03.1761.

(28) Güleç, F.; Meredith, W.; Snape, C. E. Progress in the CO2 Capture Technologies for Fluid Catalytic Cracking (FCC) Units—A Review. *Frontiers in Energy Research* **2020**, *8*, Review. DOI: 10.3389/fenrg.2020.00062.

(29) IEAGHG. *IRON AND STEEL CCS STUDY (TECHNO-ECONOMICS INTEGRATED STEEL MILL)*; 2013. https://ieaghg.org/publications/technical-reports/reports-list/9-technical-reports/1001-2013-04-iron-and-steel-ccs-study-techno-economics-integrated-steel-mill.

(30) Sulzer. *Chemtech. Structured Packings Energy-efficient, innovative & profitable*; https://www.sulzer.com/-/media/files/products/separation-technology/distillation-and-absorption/brochures/structured_packings.ashx.

(31) Michailos, S.; Gibbins, J. Effect of stripper pressure and low lean loadings on the performance of a PCC plant for 99% CO2 capture level. In Proceedings of the 16th Greenhouse Gas Control Technologies Conference (GHGT-16) 23-24 Oct 2022, 2022.

(32) IEAGHG. *Emissions of Substances Other Than CO2 From Power Plants With CCS*; 2012. https://ieaghg.org/publications/technical-reports/reports-list/9-technical-reports/1020-2012-03-emissions-of-substances-other-than-co2-from-power-plants-with-ccs#:~:text=CCS%20processes%20in%20general%20offer,some%20cases%20changes%20in%20nature.

(33) Jorgensen, T. B.; Liu, K.; Thompson, J. G. Examining the Reactions of Ethanolamine's Thermal Degradation Compounds in Carbon Capture through 1H NMR and 13C NMR. *Industrial & Engineering Chemistry Research* **2024**, *63* (25), 10863-10878. DOI: 10.1021/acs.iecr.3c04019.

Abstract Graphic